ANTIMICROBIAL MODIFICATIONS OF POLY(ETHER SULFONE) MEMBRANE

A THESIS SUBMITTED TO
THE GRADUATE SCHOOL OF NATURAL AND APPLIED SCIENCES
OF
MIDDLE EAST TECHNICAL UNIVERSITY

BY

ESRA NUR DOĞRU

IN PARTIAL FULFILLMENT OF THE REQUIREMENTS FOR

THE DEGREE OF MASTER OF SCIENCE
IN
THE DEPARTMENT OF POLYMER SCIENCE AND TECHNOLOGY

JANUARY 2016

Approval of the thesis:

ANTIMICROBIAL MODIFICATIONS OF POLY(ETHER SULFONE) MEMBRANE

submitted by **ESRA NUR DOĞRU** in partial fulfillment of the requirements for the degree of **Master of Science in Polymer Science and Technology Department, Middle East Technical University** by,

Prof. Dr. Gülbin Dural Ünver _____
Dean, Graduate School of **Natural and Applied Sciences**

Prof. Dr. Necati Özkan _____
Head of Department, **Polymer Science and Technology**

Assoc. Prof. Dr. Akın Akdağ _____
Supervisor, **Chemistry Dept., METU**

Asst. Prof. Dr. Zeynep Çulfaz Emecen _____
Co-Supervisor, **Chemical Engineering Dept., METU**

Examining Committee Members:

Prof. Dr. Levent Yılmaz _____
Chemical Engineering Dept., METU

Assoc. Prof. Dr. Akın Akdağ _____
Chemistry Dept., METU

Asst. Prof. Dr. Zeynep Çulfaz Emecen _____
Chemical Engineering Dept., METU

Prof. Dr. Pınar Çalık _____
Chemical Engineering Dept., METU

Assoc. Prof. Hasan Basri Koçer _____
Fiber and Polymer Engineering Dept., Bursa Technical University

Date: 08.01.2016

I hereby declare that all information in this document has been obtained and presented in accordance with academic rules and ethical conduct. I also declare that, as required by these rules and conduct, I have fully cited and referenced all material and results that are not original to this work.

Name, Surname : ESRA NUR DOĞRU

Signature :

ABSTRACT

ANTIMICROBIAL MODIFICATIONS OF POLY(ETHER SULFONE) MEMBRANE

Doğru, Esra Nur

M.S., Department of Polymer Science and Technology

Supervisor: Assoc. Prof. Dr. Akın Akdağ

Co-Supervisor: Asst. Prof. Dr. Zeynep Çulfaz Emecen

January 2016, 81 Pages

Fouling on a membrane is one of the major problems of liquid filtration systems. To solve this problem, physical treatments and modifications are applied on membranes. Biofouling is the most severe form of fouling, which is due to biofilms of microorganisms in a matrix of extracellular polymers they secrete. Biofilm formation has been attacked by periodic cleaning of membrane, disinfection of feed, and surface modification.

In this study, we proposed an antimicrobial surface modification to prevent biofilm formation by killing the microorganisms and inhibiting their growth. Poly(ether sulfone) (PES) based polymeric membrane was improved by chemical modification via *N*-halamines.

N-halamines are amine structures covalently bonded to halogens. In our study chlorine was used as halogen. Oxidative chlorine (Cl^+) and proton (H^+) are in an equilibrium in an *N*-halamine. *N*-halamine compounds release chlorine to a medium, and the chlorine damages the cell structure of microorganisms and kills them.

In the course of this study, the modified polymers were characterized by ATR FTIR and NMR spectrometers, which confirmed the aimed structures were obtained. The membrane performances were examined with pure water permeance measurement. The membrane morphologies were imaged by SEM. The antimicrobial activities of the membranes were examined on Gram-negative (*Escherichia coli* BL21) and Gram-positive (*Bacillus subtilis*) model organisms. It was observed that the chlorinated membranes showed biocidal activity, whereas chlorine-free membranes did not affect the growth of the bacteria on agar. Then, the *N*-halamine stability on the membranes were studied in pure water and bacterial medium (*E.coli* BL21) to predict the biocidally active span of the membranes. It was observed that increasing chlorine amount on the membrane in low bacterial concentration increases the antimicrobial effective time.

Key words: PES, membrane, *N*-halamines, antimicrobial, biofouling.

ÖZ

POLİ(ETER SÜLFON) MEMBRANIN ANTİMİKROBİYAL MODİFİKASYONU

Doğru, Esra Nur

Yüksek Lisans, Polimer Bilim ve Teknolojisi Bölümü

Tez Yöneticisi: Doç Dr. Akın Akdağ

Ortak Tez Yöneticisi: Yrd. Doç. Dr. Zeynep Çulfaz Emecen

Ocak 2016, 81 Sayfa

Membran kirlenmesi, sıvı filtrasyon sistemlerinin başlıca problemlerinden biridir. Bu sorunu çözmek için, membranlara fiziksel muameleler uygulanmakta, ve kimyasal olarak modifiye edilmektedir. Biyobirikme mikroorganizmaların hücre dışı polimerler salgılayarak biyofilm oluşturmalarıdır, ve kirlenme türlerinin en ciddisi ve en zor temizlenenidir. Biyofilm oluşumu, membranları periyodik olarak temizlemekle, stoğu dezenfektasyonla, ve yüzeye biyosidal modifikasyon ile önlenmeye çalışılmaktadır.

Bu çalışmada, antimikrobiyal yüzey modifikasyonuyla yüzeydeki mikroorganizmaları öldürerek çoğalmalarını önlemeyi, böylece biyofilm oluşumunun önlenmesi önerilmiştir. Kimyasal olarak modifiye edilmiş poli(eter sülfon)'dan membran üretip, ardından klorlanarak *N*-halamine elde edildi.

N-halaminler halojenlerle kovalent bağ içeren amin yapılarıdır. Bu çalışmada klor halojen kaynağı olarak kullanılmıştır. Yükseltgen klor (Cl^+) ve proton (H^+) denge

halindedir. *N*-halamin yapıları ortama saldıkları klorla mikroorganizmaların hücre yapılarına zarar vererek onları öldürür.

Bu çalışma sürecinde, modifiye edilmiş polimerler ATR FTIR ve NMR spektrometreleriyle karakterize edildi ve hedeflenen modifikasyonların yapıldığı teyit edilmiştir. Membran performans ve morfolojileri, saf su geçirgenliği ölçümleri ve SEM ile incelenmiştir. Membranların antimikrobiyal aktiviteleri Gram-negatif (*Escherichia coli* BL21) ve Gram-pozitif (*Bacillus subtilis*) bakteri üzerinde test edilmiştir. Agar üzerinde, klorlanmış membranlar antimikrobiyal aktivite gösterirken klor içermeyen membranlarda bakteri büyümesinde bir etki gözlemlenmiştir. Ardından, membranlardaki *N*-halaminin kararlılığı test edildi. Suda ve bakteri süspansiyonundaki (*E.coli* BL21) klor miktarı zamana karşı ölçülerek membranların antimikrobiyal aktivite gösterdiği süre öngörülmeye çalışılmıştır. Neticede, membran üzerinde artan klor miktarı, ve membranın maruz kaldığı solüsyondaki azalan bakteri konsantrasyonunun antimikrobiyal etki süresini artırdığı tespit edilmiştir.

Anahtar kelimeler: PES, membran, *N*-halaminler, antimikrobiyal, biyokirlenme.

To my dear family

ACKNOWLEDGMENTS

I would like to express my deepest gratitude to my supervisors, Dr. Akın Akdağ and Dr. Zeynep Çulfaz Emecen for providing me with support, invaluable guidance, encouragement, patience, and suggestions.

I also thank my team members in Akın Akdağ Research Group and Membranes for Liquid Seperations Group for their friendship and support during my study; Duygu Tan, Elif Nur Durmaz, Gizem Çalışgan, Gizem Tekin, Halil İpek, Hazal Yücel, Kaan Bolat, Kıvanç Akkaş, Milad Fathi, Faqih Muhamad Sukma, Perihan Öztürk, Sibel Ataol Türkkan, Yiğit Gençal.

I would like to thank Prof. Dr. Pınar Çalık for giving me opportunity to use her laboratory for antimicrobial tests. Also I would like to thank her research group members, especially Özge Ata Akyol, Hande Güneş, Sibel Öztürk, Aslan Massahi for their kindness and support. I thank Prof. Dr. Halil Kalıpçılar, Asst. Prof. Dr. Erhan Bat, and their research members for providing to use their laboratories during my research. I thank Prof. Dr. Ülkü Yetiş and Mert Erkanlı for their experimantal support and help. I thank Yusuf Samet Aytekin and Adem Yavuz for their support for experiments.

I thank METU, especially Chemistry and Chemical Engineering Departments for providing to learn and to research opportunity.

I would like to thank my parents for their great support and patience during all my education and especially for their lifetime effort on me.

I thank my grandmothers, from whom I have learnt to read, and to live decent, and I thank my siblings, nephew and nieces, aunts and uncles, cousins, and everyone makes my life so delighted.

I thank all my friends in my life, they are whom I've have fun and sorrow, and I have being grown up with.

I thank Sefa Şimşek changing my life and make it lovely.

TABLE OF CONTENTS

LIST OF FIGURES

LIST OF TABLES

NOMENCLATURE AND ABBREVIATIONS

PES	: Poly(ether sulfone)
PES-NO_2	: Funtional nitro group grafted on poly(ether sulfone) backbone
PES-NH_2	: Funtional amine group grafted on poly(ether sulfone) backbone
PES/PES-NH_2	: Membrane prepared from the dope solution of 10% PES and 6% PES-NH_2 dissolved in 84% *N*,*N*-dimethylformamide (DMF)
PES-NHAc	: Functional amide group grafted on poly(ether sulfone) backbone
PES/PES-NHAc	: Membrane prepared from the dope solution of 10% PES and 6% PES-NHAc dissolved in 84% *N*,*N*-dimethylformamide (DMF)
PES/PES-NCl_2	: Chlorinated form of PES/PES-NH_2 membrane
PES/PES-NClAc	: Chlorinated form of PES/PES-NClAc membrane
DMF	: *N*,*N*- dimethylformamide
NMP	: *N*-methyl 2- pyrrolidinone
THF	: Tetra hydrofuran
ATR FTIR	: Attenuated Total Reflectance Fourier Transform Infrared Spectrometer
NMR	: Nuclear Magnetic Resonance Spectrometer
SEM	: Scanning Electron Microscope
MF	: Microfiltration
UF	: Ultrafiltration
NF	: Nanofiltration
RO	: Reverse osmosis
DMSO-d_6	: Deuterated dimethylsulfoxide

LB	: Lysogen broth
CFU	: Colony forming unit
PBS	: Phosphate buffered saline
TFAA	: Trifluoro acetic anhydride

CHAPTER 1:

INTRODUCTION

A membrane is a selective barrier between two phases [1-3]. Depending on the membrane structure, membranes can be classified as nonporous and porous membranes [2]. Nonporous membranes are dense films in which transport and seperation occur via solution-diffusion mechanism**.** Porous membranes are classified depending on the pore sizes (Table 1) as nanofiltration, ultrafiltration, and microfiltration membranes [1]. In this thesis, polymeric porous ultrafiltration membranes were studied.

Table 1. Membrane process, pore size range, and example species retained.

Process	Pore size range	Examples of species retained
Microfiltration (MF)	> 0.1 μm	Bacteria, suspended solids
Ultrafiltration (UF)	10 – 100 nm	Viruses, macromolecules, colloids
Nanofiltration (NF)	1-10 nm	Small organics, multivalent ions
Reverse osmosis (RO)	nonporous	Monovalent ions

Ultrafiltration membranes are widely used for seperation and purification processes since their fabrication in integrally skinned form by Loeb and Sourirajan in 1960s [1]. Average pore diameter of ultrafiltration membranes is in the range of 10-100 nm. They typically have an anisotropic structure [1, 2, 4], which means they have thin selective skin layer, and a thicker support layer underneath. Skin layer has smaller pore size than the support layer, therefore it determines the selectivity. Support layer has a microporous structure with high permeance. This layer serves as mechanical support for the membrane [1]. The entire thickness of the ultrafiltration membranes are several hundreds of micrometers, whereas the selective layer thickness is

generally less than 1 μm. Since the selective layer is so thin, the anisotropic membranes have higher flux compared to isotropic membranes of the same overall thickness. These thin selective layers can withstand operation pressures (*ca.* 1-10 bar) due to the macroporous support beneath [2].

Polymeric ultrafiltration membranes are mostly prepared by the phase inversion method. Phase inversion is a process in which the polymer is transformed from liquid solution to solid precipitate [2, 4]. Typical procedure of phase inversion is casting a dope solution (membrane material dissolved in a proper solvent) on a substrate, and then precipitating the polymer by immersion of the polymer solution in the non-solvent. The process is called immersion precipitation [1, 4].

A polymer should have certain properties to be used as a membrane via this technique. A must of those properties is having a proper solvent to dissolve, and a proper non-solvent to coagulate, where the solvent and non-solvent are fully miscible in each other [1]. Furthermore, an ideal polymer is tough, amorphous but not brittle, thermoplastic, with glass transition temperature higher than 50^{o}C above the usage temperature [1]. The molecular weight of the polymer should be more than 30 kDa [1]. Depending on the expected facilitation conditions, mechanical, thermal strengths, chemical and pH stability may be other requirements of the polymer. Poly(ether sulfone), poly(sulfone), poly(imide), poly(acrylonitrile), poly(phenylene sulfide), poly(etheretherketone), cellulosic polymers, aliphatic polyamides are some of the materials used for ultrafiltration membranes [2, 4].

In this study, poly(ether sulfone) (PES) is the membrane polymer. PES is a widely used as an engineering plastic. It shows excellent chemical, thermal, and mechanical properties. Furthermore, aromatic rings in the polymer chain allow us to chemically modify the polymer [5-7].

The casting solvents are usually aprotic solvents, such as *N*,*N*-dimethyl formamide, *N*-methyl pyrrolidone, dimethyl acetamide. Casting solutions with low solubility parameter solvents, such as tetrahydrofuran, acetone are usually not proper for rapid precipitation [1].

The precipitation is provided by a non-solvent. The non-solvent should be miscible with the solvent, and it should precipitate the polymer. Any medium meeting those necessities can be used. Yet, water is almost always used as precipitation medium, since it is almost free, easily accesible, and also its vapor is safer to work with compared to organic-based solvents such as methanol or isopropanol [1].

Modifiers can also be used to change the properties of the membranes, such as membrane structure and performance. Weak or strong non-solvents, co-solvent, salts, hydrophilic or amphiphilic polymers, and surfactants are widely used modifiers. The modifiers change the interaction between the solution and non-solvent, and change the coagulation path of the solution. Some of the additives can be partially or totally removed by washing [1], while some remain as a part of the matrix or accumulate on the surface.

The performance of the membrane varies with the porosity, pore structure, size and distribution, and the hydrophilic character of the membrane material [8]. As it was mentioned above, the structure of the membrane is varied with the elements of dope solution and coagulation medium.

After the casting the dope solution on a substrate, the solution precipitates in a non-solvent. The composition and phase change of the polymer in a polymer-solvent-nonsolvent system is represented by ternary phase diagram (Figure 1 [8]). The corners of the triangle represent the pure components of polymer, solvent and non-solvent. The corners and the points within the triangle represent mixtures of the components. On the phase inversion path of the polymer solution, the mixture loses solvent and gains non-solvent. During the solvent exchange, the mixture first stands in the one-phase region, then gets into the two-phase region. At the end of the phase inversion, the polymer includes no solvent in it, and takes the solid form. During the process, concentration and concentration gradient of the solution differ on each part of the membrane in each moment. The mixture in the one-phase region is a homogenuous solution. Phase separation occurs by nucleation and growth between binodal and spinodal boundry, in metastable region. Within the spinodal region the composition is unstable and phase separates via spinodal decomposition. In either

path the mixture separates into two; polymer-rich phase, which eventually forms the membrane, or polymer-lean phases, which forms the pores [8].

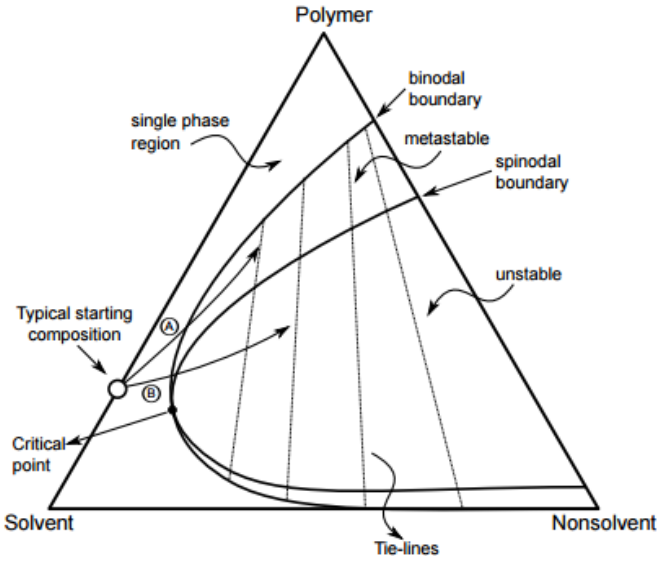

Figure 1. Ternary phase diagram. Path A shows phase inversion via nucleation and growth, Path B is via spinodal decomposition.

The skin layer determines the performance ultrafiltration membrane, which is described by permeance and retention of compounds in the feed [8].

In Figure 2 cross-flow membrane process is demonstrated. Permeate flux is the passed amount of permeate through the membrane per unit time, per membrane area. Permeance is the permeate flux per unit trans membrane pressure difference (P_{feed}-$P_{permeate}$). Retention is the ratio of the difference of feed concentration and permeate concentration to the feed concentration. If the concentrations are equal to one another, this means that there is no retention. If the permeate concentration is equal to zero, R=100%.

Permeate flux, permeance and retention are calculated with the following equations, respectively.

$$J = \frac{V}{A.t} \quad ; \quad Permeance = \frac{J}{\Delta P} \quad ; \quad R = 1 - \frac{C_P}{C_F}$$

where J is permeate flux, V is volume of permeate, A is the membrane area, t is permeation time, ΔP is trans membrane pressure difference, R is retention, C_P is permeate concentration, C_F is feed concentration.

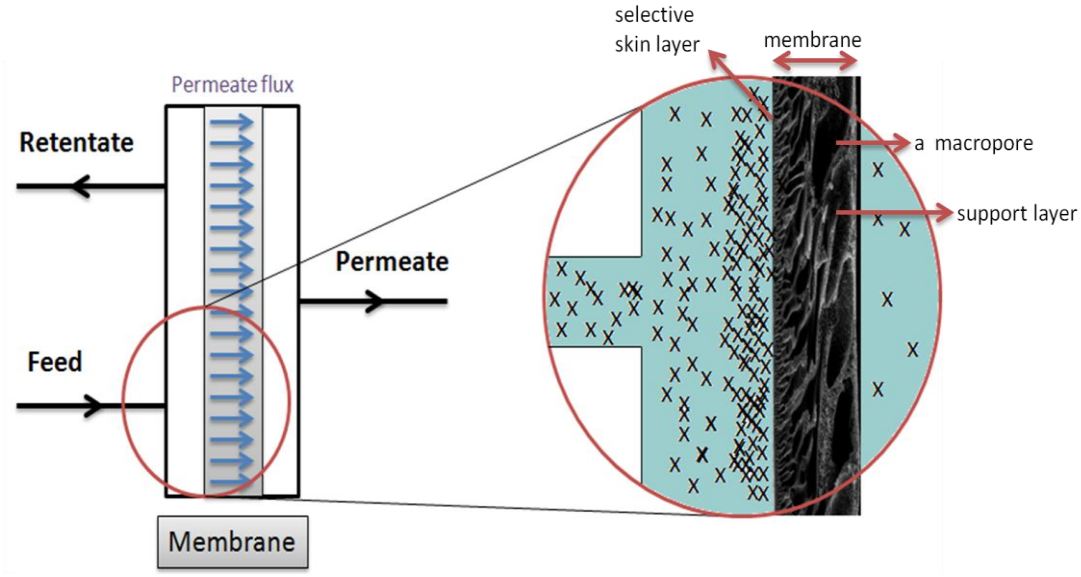

Figure 2. Demonstration of a cross-flow membrane module separation.

Skin layer thickness and pore size determines the permeance and retention. Thin skin layer provides a high flux per trans membrane pressure, *i.e* permeance. Increasing pore size increases the permeance, while it decreases the retention of a given compound.

The concentration of retained solutes increases near the membrane surface during filtration (Figure 3). This concentration build-up generates back-diffusion to the bulk of the feed. This is called concentration polarization. The concentration profile establishes a steady-state in the boundry layer. In this case the convective transport of solute towards the membrane is equal to the sum of the permeate flow and the diffusive back transport of the solute [1, 2, 8].

$$J \,.\, c + D \,.\, \frac{d_c}{d_x} = J \,.\, c_p$$

where J is the permeate flux, c is the particle volume fraction in the concentration polarization layer, c_p is the particle volume fraction of the permeate, D is the

diffusion coefficient of the particle in the solvent and *x* is the coordinate perpendicular to the membrane surface [8].

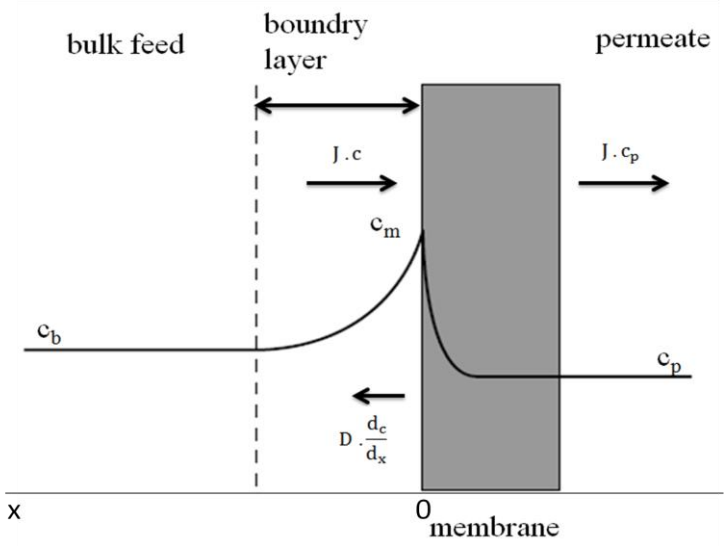

Figure 3. Concentration polarisation profile.

When the concentration at the membrane surface is high enough to cause precipitation of the retained solute, concentration polarization results in deposition on the membrane surface, which is one components of membrane fouling. Membrane fouling is the deposition of retained particulates, macromolecules, salts, bacterial substances on and/or in the membrane.

Concentration polarization and fouling decrease the permeate flux in time. In dead-end operation, all retained solutes continuously deposit on the membrane surface. In the cross-flow operation, the feed flows through the membrane to permeate, and tangential to the membrane to retentate (Figure 4). Providing this cross-flow decreases the concentration polarization but increases the operating costs and system complexity [2].

Other than particle fouling, bacterial fouling results in formation of biofilms (biofouling), which is not solved with cross-flow operation in a long term. Lewandowski and Beyenal define biofilm as *"An aggregate of microorganisms imbedded in a matrix composed of microbially produced extracellular polymers and attached to a surface"* [9]. The biofilm formation consists of three stages. First, the microorganisms attach to the surface, then they colonise and grow on the surface.

There are mainly three strategies to prevent biofilm formation on membranes by modifying the membranes used: obtaining bacteria-resistant, bacteria-releasing, or biocidal surfaces [10].

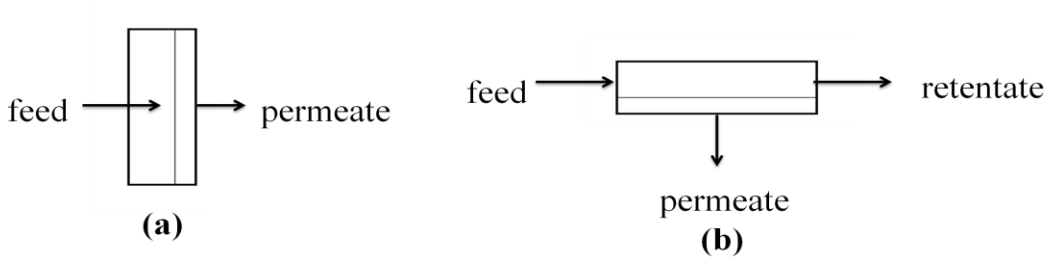

Figure 4. Dead-end (a) and cross-flow (b) membrane operations.

Bacteria-resistant surfaces reduce the bacterial attachment to the surface. It is used to prevent early stages of biofilm formation. It is assumed that blocking the initial attachment of the bacteria to the surface prevents the non-specific interactions with the biological environment, *i.e* proteins. These surfaces are obtained usually with hydrophilic compounds, such as ethylene glycol based [11], and zwitterion based [12] groups.

Bacteria-releasing surfaces allow the initial attachment and growth of the bacteria, however release them under proper conditions. Low surface energy silicone and fluorine based polymers exhibit such bacteria-release property. Lowering hydrogen bonding and polar interactions lower the adhesion strength, therefore fouled microorganisms are released from the surface by shear application. For this purpose, stimuli-responsive surfaces are also studied [13]. Those materials change the physicochemical properties depending on the environmental stimuli, *i.e* temperature, pH, ionic strength, light, etc. After fouling occurs, the environment of the surface changes such that the surfaces swell or shrink thereby repelling the bacteria from the surface [10].

Lastly, biocidal surfaces are used for antimicrobial purposes. Biocidal refers to compounds killing the microorganism. Killing mechanism of the biocidal compounds can be direct damaging to cell structure, or intoxicating the cell [14]. This approach has been used in this study.

Yu et al. divides biocidal surfaces into two: contact-based or release-based [10]. Contact-based surfaces are defined as antimicrobial agents that kill the microorganism adhered, whereas release-based surfaces are defined as those that slowly release antimicrobial agents to environment to kill the microorganism [10]. Silver nanoparticles [15, 16], quaternary ammonium [17] and phosphonium [18] compounds are widely used biocidal sources.

In this thesis, *N*-halamines are used as the biocidal source. *N*-halamines were proposed as a chlorine source first by Kovacic et al. in 1960s [19, 20]. An *N*-halamine can be defined as a compound containing nitrogen-halogen covalent bonds (Figure 5). The nitrogen can be in the form of amine, amide, or imide (Figure 6), while the halogen can be chlorine, bromine, or iodine [21].

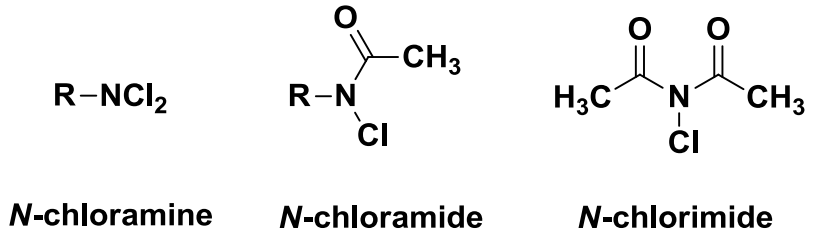

Figure 5. The *N*-halamine structures.

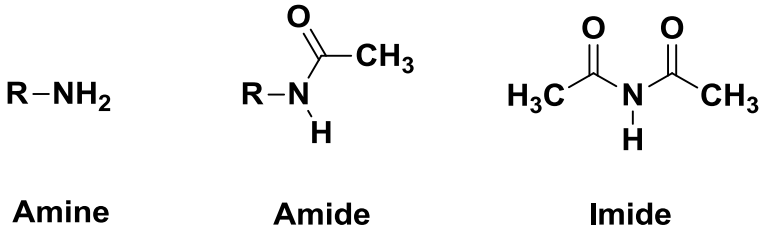

Figure 6. The structures of amine, amide, and imide functional groups.

N-halamines are widely studied and used for biocidal purposes. They are effective against broad spectrum of microorganisms: Gram-negative, Gram-positive, drug-resistant bacteria, viruses, fungi [21-23]. Also, N-halamines are regenerable, safe to environment, and have long-term stability in air and in water [21]. Due to these unique properties, *N*-halamines are extensively used in water disinfection and purification [23-25], textiles [26], paints [27], and drug studies [28].

The biocidal activity of *N*-chloroamines is exploited by nature. For this purpose, in humanbody there exists an amino acid called taurine. Taurine is 2-aminoethanesulfonic acid. It comprises almost 0.1% of body weight in most mammalians, whereas almost none in bacteria and plants [29]. It is chlorinated or brominated *in-vivo* and the chlorinated taurine (TauCl) and the brominated taurine (TauBr) are used to fight foreign pathogens by indigenious cells [29-31].

The biocidal working principle mechanism of the *N*-halamines is dissociating a halogen in "+1" oxidation state to aquous medium to form hypohalous acid as shown in Figure 7.

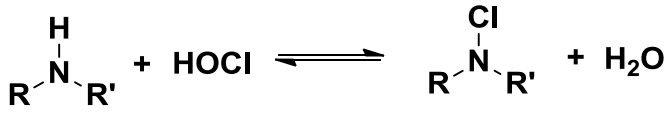

Figure 7. The equilibrium of amine, *N*-chloroamine and hypochlorous acid in water.

The biocidal efficiency of an *N*-halamine can depend on the stability of nitrogen containing group (amine, amide, and imide) (Figure 6), efficacy of halogen, effecting rate and span, and rechargability.

The stabilities of halogen on different nitrogen containing compounds are different in air and aquous medium. Primary amine compounds are not stable in air. They are oxidized to nitro compounds [32]. Imide compounds undergo rapid hydrolysis in water. Amide is stable in air and water medium [21].

Those nitrogen containing groups shown in Figure 6 are for acyclic structures. Such *N*-chloramine groups on aromatic rings are prone to oxidation, therefore they release "Cl^+" more rapidly than the *N*-arylamides. The studies show that biocidal activity and stability of amide *N*-halamine compounds increase in cyclic compounds compared to acyclic compounds [21, 22, 33].

In *N*-halamine compounds mostly chlorine is used as the halogen, but bromine and iodine can be also used [21]. It is reported that *N*-bromamines are more effective than analogues of *N*-chloramines [19]. However, sodium hypochlorite, which is the

chlorination source, is widely used as industrial, house and swimming pool disinfectant, easy to obtain, and cheap material. Therefore, *N*-chloroamines are the mostly widely studied and used *N*-halamines. Besides chlorine and bromine, there are few studies on *N*-iodoamines in literature [28, 34].

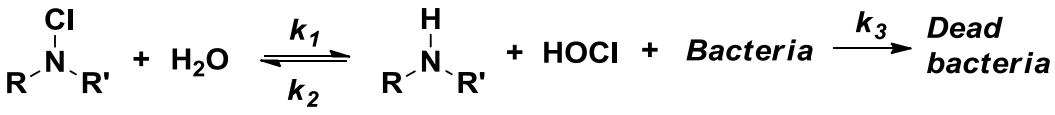

Figure 8. The kinetic reaction equation of *N*-chloroamine in bacterial medium.

The biocidal action time is related with the dissociation of biocial agent, *e.g N*-halamine in water dissociates to hypochlorous acid and corresponding nitrogen compound. The dissociation of chlorine and killing bacteria is shown in Figure 8. Equilibrium constant ***K*** is the ratio of forward and reverse equilibrium rates, $K=k_1/k_2$. Increasing ***K*** increases HOCl concentration in the medium. On the other hand, k_3 is not included into the equilibrium calculation because it is irreversible. That implies the interaction of bacteria and HOCl is irreversible, yet the stoichiometry is unknown. The dissociation constants of *N*-halamines are in the order of imide > amide > amine (with the *K* values of the order of 10^{-4}, 10^{-9}, and 10^{-12}, respectively) [33]. It can be concluded that imide provides fastest biocidal activity, whereas amine does the slowest.

The effective contact time of *N*-halamines are examined by numerous research groups. The effective contact time per microorganism concentration can alter for each type of microorganism. *E. coli* is one of the most used model bacteria. It is reported that contact time less than 1 s/mL result in dead *E. coli* [21, 24]. Lasting biocidal efficacy is not much examined by research groups. However, Worley et al. reported that after 15 min contact time with derivatives of *N*-halaminated polystyrene hydantoin all bacteria were dead, whereas after 30 min and more contact time the amount survived bacteria increases gradually [24]. One can conclude that halogens are consumed relatively a few time and loose antimicrobial activity. However, they can be regenerated repeatedly.

The stability and usability of *N*-halamine compound is also related with not only amine groups, but also neighbouring atoms. If amine is connected to a carbon which constitutes hydrogen(s), dehydrohalogenation yields an imine after the halogenation [21, 35]. That causes lost in function of biocidal activity.

The driving force of dehydrohalogenation can be basic medium, or UV light or heat. The reactions of dehydrohalogenation are shown in Figure 9. With this in mind, compounds structural integrity will be lost. Therefore, amines and amides nitrogens should be bonded to the carbon atoms on which hydrogen should be absent.

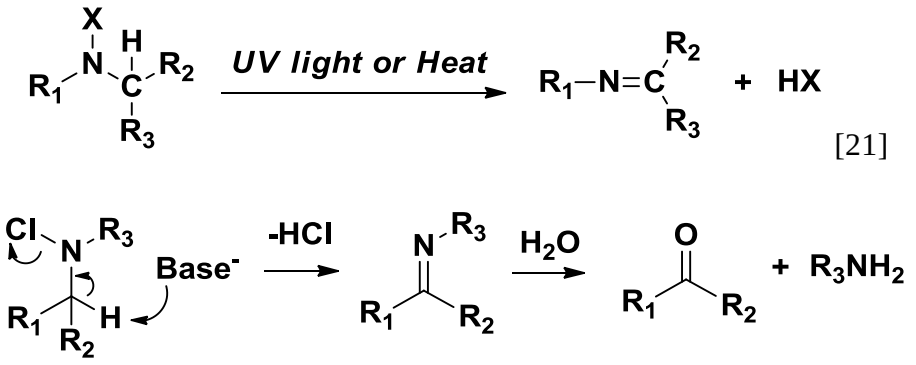

[21]

Figure 9. Dehydrohalogenation reactions with base, UV light or heat.

There are several studies on *N*-halamines. Various nitrogen containing molecules and polymers were synthesized. The antimicrobial efficacy of those compounds were examined with different halogens. The products are also examined on antimicrobial surfaces, textiles, paints, and membranes.

Worley et al. studied on the performances of *N*-chloroamines and *N*-bromoamines on analog conditions. They loaded chlorine and bromine on polystyrene hydantoin, then examined the biocidal behaviour of the materials varying pH, temperature, flow rate conditions. They reported that free chlorine and bromine are more effective than *N*-chloroamine and *N*-bromoamine. However, they indicated that although free chlorine content is affected by variations in pH, *N*-halamines are similarly effective at acidic, basic and neutral conditions. The temperature change affects the biocidal efficacies of the *N*-chloroamine, whereas *N*-bromoamine is not affected. That is because the chlorine hydrolyses less at low temperatures, but there is not a significant decrease in

hydrolysis of bromine. They examined the effect of flow rate also. They reported that both *N*-halamines are effective even at high rates [24].

N-halamines are used on textile. Worley et al. studied an antimicrobial cotton with *N*-halamines. They coated the cotton with two different funtional groups in Figure 10 [26]. Then chlorinated the modified cotton to achieve antimicrobial activity. They tested the chlorination of the modified cotton after washed several time, and reported that the product was still getting chlorinated after 50 cycles of washes [26].

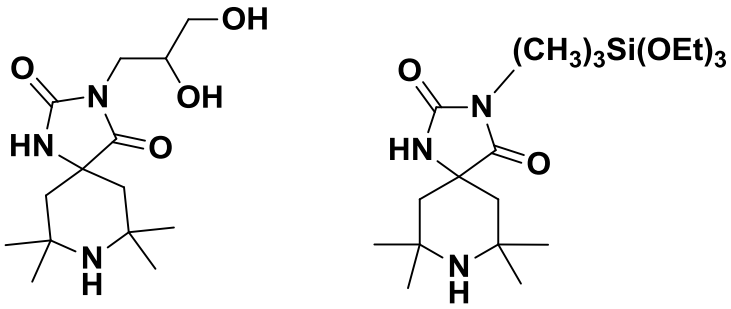

Figure 10. The compounds studied for modification.

Sun et al. studied this phenomenon on an antimicrobial paint. For this purpose, they produced polymeric *N*-halamine latex emulsions into water-based latex paints. The starting and final compounds of the reaction are shown in Figure 11 [27].

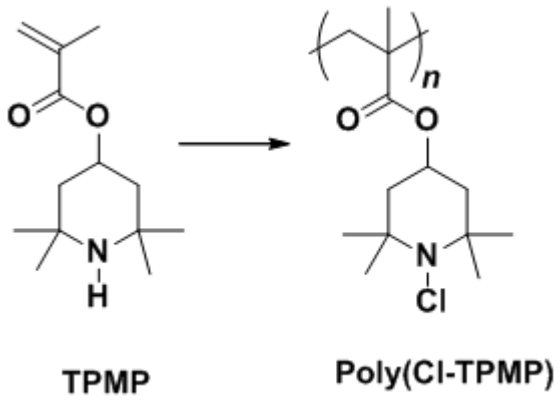

Figure 11. Monomer tetramethyl-4-piperidyl methacrylate (TMPM), and polymer poly(chloro- tetramethyl-4-piperidyl methacrylate) (Poly-Cl-TMPM).

They examined the biocidal and biofouling activity of the paint film, and reported the compound is effective on bacteria. Also, the biofilm formation was succesfully

prevented. They stated that the antimicrobial activity is easily monitored with iodine/starch test. If the antimicrobial activity of the paint was lost, it could be regenerated. They reported the chlorine content was essentially unchanged after 10 cycles of recharge treatment [27].

Ahmed et al. studied on modification of polyepichlorohydrin to cross-linked polyepicyanuriohydrin (Figure 12) [23] to obtain antimicrobial polymer. They made the antimicrobial analysis in lab scale and reported the polymer kills *E.coli* and *S.aureus* bacteria and bacteriophage PRD1 virus. They also suggested a large scale application of the process [23].

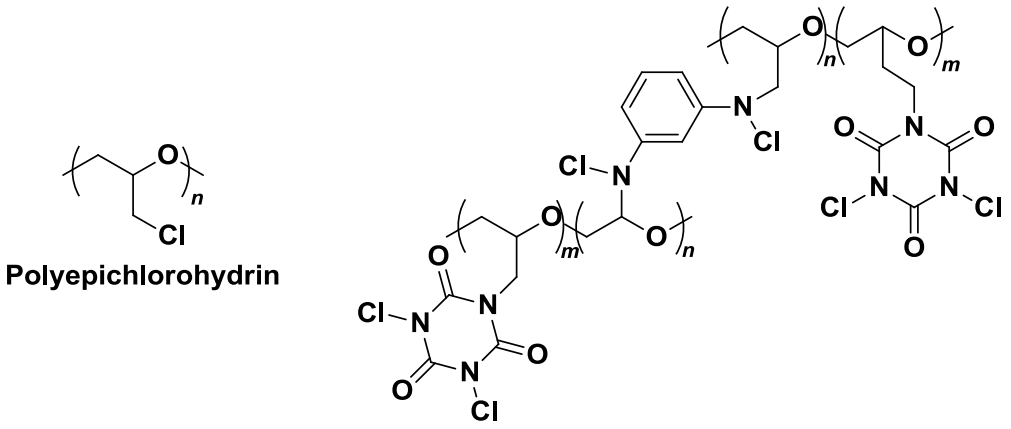

Figure 12. Nascent and cross-linked polyepicyanuriohydrin.

N-halamines have been considered in membrane applications as well. Wang et al. studied biofouling and the chlorine resistance properties of a commercial aromatic polyamide membrane improved by *N*-chlorinated carbodiimide-induced grafting with imidazolidinyl urea (IU). The brief version of the reaction is shown in Figure 13 [25]. They examined the biofouling properties of the membranes by measuring the pure water flux before and after the exposure to *E.coli*. They reported that there was small decrease in flux of modified membrane, whereas the unmodified membrane demonstrated a dramatic decrease. Besides, the chlorine resistance is an important property of polyamide membranes, since, as it was mentioned before, regular cleaning of the membranes are made usually with chlorine. This causes a neccessity

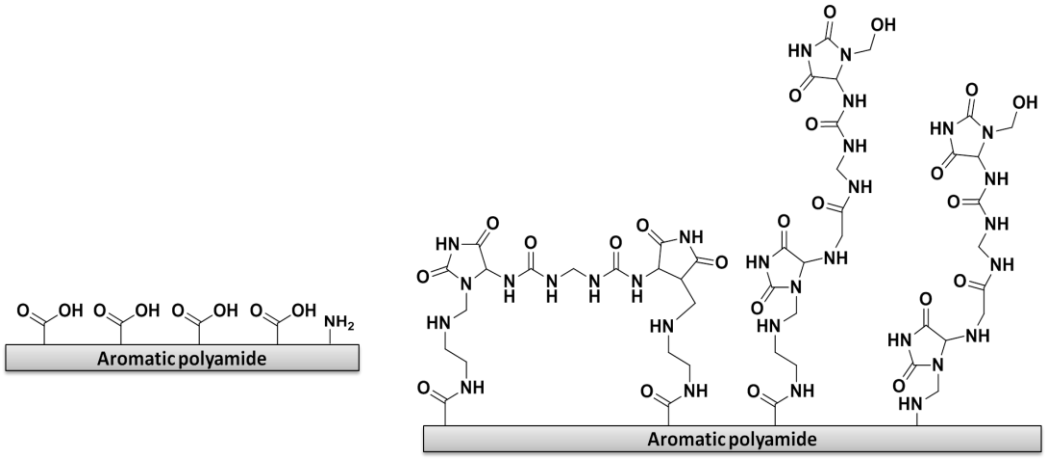

Figure 13. The nascent and modified membranes.

that the membranes be resistant to chlorine in long term. To examine the chlorine resistance, the initial water flux of the membranes were measured. The membranes contacted with *E.coli* suspension, then chlorinated, and the water flux was measured again for three cycle. They reported that the water fluxes of the membranes after chlorination and re-chlorination were not significantly different [25].

Zhang et al. studied on hydrophilic PES ultrafiltration membrane containining "SiO_2@*N*-halamine" nanoparticles. They modified silicon oxide nanoparticles to get SiO_2@*N*-halamine, the modified molecule is shown in Figure 14 [36]. Afterwards, hybrid SiO_2@*N*-halamine/PES membranes were prepeared. It was reported that the hydrophilicity of the membane increased with increasing SiO_2@*N*-halamine nanoparticle content. They also tested the membrane for antimicrobial purposes, and reported the hybrid membrane showed antimicrobial activity [36].

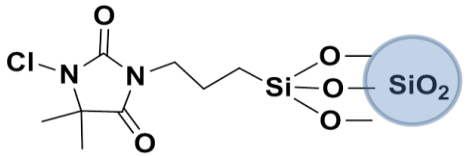

Figure 14. SiO_2@*N*-halamine nanoparticle.

In this thesis, we aim at manufacturing *N*-halamine containing membrane and running performance and biocidal test for the new membrane.

To start with this general idea, we use poly(ether sulfone) (PES) as a base polymer. This polymer is chosen because of its wide use in membrane production. PES is nitrated, then the nitro group is reduced to amine. This amine is chlorinated and tested for the membrane tests. Another modification is to acetylate those amino groups into amide functionalities. The general idea is summerizaed in Figure 15. The membranes' antimicrobial performances were tested. This study will provide novel paths to antibiofouling membranes.

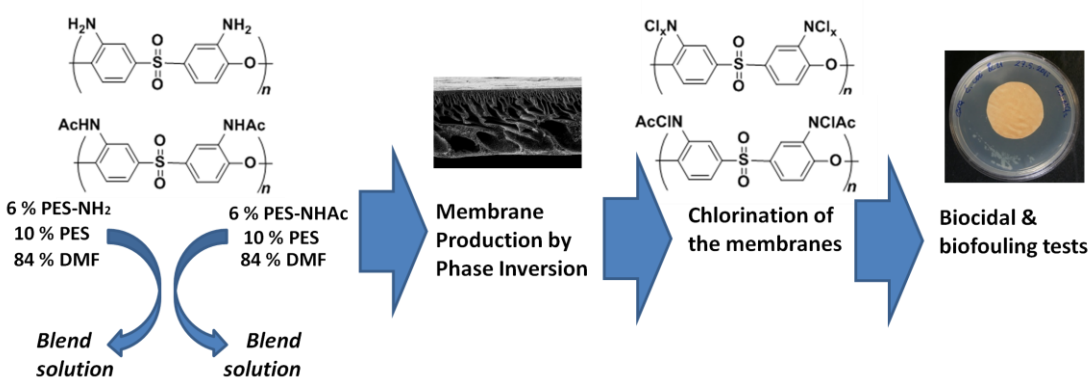

Figure 15. Flow chart of this study.

CHAPTER 2:

EXPERIMENTAL

2.1. Materials and instruments

Poly(ether sulfone) (PES, Ultrason E6020P) was supplied by BASF. Deuterated dimethylsulfoxide (DMSO-d_6) (99.8%), *N*,*N*-dimethyl formamide (DMF) (99.8%), sulfuric acid (H_2SO_4) (95-97%), acetic acid (CH_3COOH) (100%), acetic anhydride ($(CH_3CO)_2O$) (98.5%), LB Broth (Miller) were purchased from Merck. Hydrochloric acid HCl (36.5-38%), glutaraldehyde (25%), phosphate buffered saline, ethanol (99.8%), ammonium nitrate (NH_4NO_3) (98%), trifluoro acetic anhydride (TFAA) (99%), phenylhydrazine (97%), nitric acid (HNO_3) (65%), sodium acetate (NaOAc) (99%), triethylamine (Et_3N) (99%) were purchased from Sigma-Aldrich. Tin (II) chloride ($SnCl_2$) was Riedel-de Haen Ag Seelze-Hannover.

Tap water was used as coagulant. Ultrapure water (18 MΩcm) was used in membrane permeance measurements. The instruments used for the analysis are; ^{1}H NMR Spectrometer is Bruker Ultrashield 400, UV-Vis Spectrometer is Shimatzu 1600, ATR FTIR is Bruker Alpha, contact angle instrument is Attension TL101, SEM is Quanta 400F Field Emission SEM.

2.2. Chemistry

2.2.1. Modification reactions

2.2.1.1. Nitration

PES (**1**, FTIR: 1483, 1575 cm^{-1}. NMR: 7.27, 8.00 ppm) was dissolved in proper solvents in 250 mL flasks. The acids and, if exist, the solvents were poured slowly on the solution. The mixture left to react at particular temperatures for particular time intervals (see Table 2). The product, PES-NO_2 (**2**), was washed and dried with distilled water, ethanol, and diethylether, respectively. The reaction progress was

monitored by FTIR. The product was characterized by ATR FTIR (Appendix Part A) and NMR spectrometers.

Table 2. Nitration reaction conditions and appeared characteristic peaks.

Proc.	PES amount (g)	Solvent	Reactants	Time (h)	Temp. (^oC)	FTIR wavenumber (cm^{-1})	NMR Chem. shifts δ (ppm)
a [7]	10	-	30 mL $HNO_{3(aq)}$ and 40 mL $H_2SO_{4(aq)}$	6	65	1535	7.68, 8.41, 8.84
b [5]	1.5	10 mL DCM	0.25 g NH_4NO_3 and 3.2 mL TFAA	24	0 to rt	1536	*
c [37]	5	110 mL $C_6H_5NO_2$	80 mL $HNO_{3(aq)}$ and 20 mL $H_2SO_{4(aq)}$	18	0 to rt	No characteristic peak appeared.	*
d	3	60 mL DMF	50 mL $HNO_{3(aq)}$ and 12 mL $H_2SO_{4(aq)}$	18	rt	1528	*

* Further structural with ^1H NMR analysis of these products were not measured.

2.2.1.2. Reduction

PES-NO_2 (product **2**, procedure **a**) was mixed with solvent, reactant, and catalyst to obtain PES-NH_2 (**3**). The mixture was left to react at particular temperature and

Table 3. Reduction reaction conditions and appeared characteristic peaks.

Procedure	PES-NO_2 amount (g)	Solvent	Catalyst	Time (h)	Temp. (^oC)	FTIR wavenumber (cm^{-1})	NMR Chem. shifts δ (ppm)
a [7]	10	50 mL EtOH	20 g HCl, 20 g $SnCl_2$	4	65^{o}C	3350	5.57, 6.80, 6.99, 7.27
b	3	-	90 mL phenylhydrazine	20	120 ^{o}C	1590, 3350	**
c*	3	30 mL EtOH	0.3 g Pd/charcoal	4	80 ^{o}C	-	**

* This reaction was run at 64 bars.

** Further structural with ^1H NMR analysis of these products were not measured.

pressure for particular time intervals (Table 3). The product was washed and dried with distilled water, ethanol, and diethylether, respectively. The product was characterized by ATR FTIR (Appendix Part A) and NMR spectrometers.

2.2.1.3. Acetylation

PES-NH_2 (product **3**, procedure **a**) was mixed with solvent, and reactant(s). The mixture was left to react at particular temperature and pressure for particular time intervals (see Table 4). The product was washed and dried with distilled water, ethanol, and diethylether, respectively. The reaction progress was monitored by FTIR. The product was characterized by ATR FTIR (Appendix Part A) and NMR spectrometers.

Table 4. Acetylation reaction conditions and appeared characteristic peaks.

Proc.	PES-NH_2 amount (g)	Solvent	Reactant(s)	Time (h)	Temp. (^oC)	FTIR wavenumber (cm^{-1})	NMR Chem. shift δ (ppm)
a	5	-	50 mL CH_3COOH	18	rt	1673, 3300	2.1
b	2	30 mL water	10 mL HCl, 5 g NaOAc	12	0	1682, 3300	*
c	2	5 mL DMF	3 mL $(C_2H_5)_3N$, 3 mL $(CH_3CO)_2O$	12	rt	1771	*

* Further structural with ^1H NMR analysis of these products were not measured.

2.3. Membrane

2.3.1. Membrane preparation

PES was dried at 80^{o}C, modified PESs dried at 30^{o}C before use. For pristine PES membrane, 10 wt % PES was dissolved in 90 wt % DMF. For modified PES membranes; 6 wt % modified polymer was first mixed with 84 wt % DMF. The solution was ultrasonicated for 2-3 min. After getting a homogenuous solution, 10 wt % PES was added into the solution, and the mixture was left to mix on roller-mixer. The blend mixture was filtered with 300 mesh commercial filter to get rid of any dust or undissolved particles. The solutions were cast on a glass substrate with 250 μm

thickness. Cast solution on the substrate was immersed in a 6 liter tank filled with tap water as coagulant at room tepmerature. The water refreshed in the first hour of coagulation. After 24 hours washing, the membranes left to dry in room temperature.

2.3.2. Membrane chlorine assessments

2.3.2.1. Chlorination

Sodium hypochlorite (NaOCl) solutions including 1, 3, 5, 10, 15 % of active chlorine were prepared and pH was adjusted to 7 by acetic acid. PES/PES-NH_2 and PES/PES-NHAc membranes were exposed to the solution for 1, 10, 30, 60 min at room temperature to get PES/PES-NCl_2 and PES/PES-NClAc. Then, the chlorine amounts loaded on membranes were determined with iodometric titration (see Appendix Part C).

2.3.2.2. Chlorine release

The chlorinated membrane coupons were exposed to pure water and bacterial solutions in a cross-flow cell, with cross flow of feed at a rate of 15 mL/min. Once in a while a coupon was taken from the medium and chlorine amount was determined by iodometric titration. (see Appendix Part C)

$$OCl^- + 3I^- + 2H^+ \xrightarrow{starch} Cl^- + I_3^- + H_2O$$

$$I_3^- + 2\,S_2O_3^{2-} \xrightarrow{starch} 3\,I^- + S_4O_6^{2-}$$

The chlorine amount is calculated as:

$$n_{Cl^+} = \frac{V_{NaS_2O_3} * M_{NaS_2O_3}}{2} * Mw_{Cl}$$

where n_{Cl^+} is mole of active chlorine, $V_{NaS_2O_3}$ is volume of the titrant NaS_2O_3, $M_{NaS_2O_3}$ is molarity of the titrant, Mw_{Cl} is atomic weight of the chlorine.

2.3.3. Membrane characterization

2.3.3.1. SEM

The surface and cross-section of membranes were analyzed with Scanning Electron Microscope (SEM). The membrane samples were coated with palladium-gold to achieve the conductivity.

2.3.3.2. Contact angle measurement

The hydrophilicity of the membrane surfaces were examined with deionized water by sessile drop method of contact angle measurement.

2.3.3.3. Membrane performance assessments

Pure water permeance was measured in a cross-flow cell operated at constant flux by measuring Trans Membrane Pressure (TMP) required to sustain the imposed flux. Measurements were taken at three fluxes, and the slope of the flux vs TMP graph was given as the membranes' pure water permeance.

2.4. Biological properties

2.4.1. Biocidal assessments

2.4.1.1. Static biocidal assessments

Static biocidal assessments were done on Gram-negative (*Escherichia coli* BL21) and Gram-positive (*Bacillus subtilis*) bacteria. The bacteria were incubated in seperate LB Broth (20 g /L) liquid nutrient mediums. Depending on the growth curve analysis (Appendix Part D), 10 µL of 10^9 CFU/mL bacteria were inoculated on LB Agar (35 g/L) solid nutrient medium. The membrane coupons sterilized with ethanol and sterile ultra pure water, respectively, were placed on the bacteria. In order for bacteria to grow, the media were incubated for 24 h at 37^{o}C. Then, inhibition zones of the bacteria were examined.

2.4.1.2. Kinetic biocidal assessments

Kinetic biocidal assessment was done on Gram-negative (*E. coli* BL21) bacteria. The bacteria were incubated in LB Broth (20 g/L) liquid nutrient medium. Depending on the growth curve analysis, an empty set without any membrane, and two seperate sets chlorinated membrane coupons (PES/PES-NCl_2 and PES/PES-NClAc) were put in bacterial solution during the exponential phase. 10 µL bacterial solution was taken once in every 90 min and inoculated on LB Agar medium for incubation for 24 h at 37^{o}C. The membrane colonies formed were observed.

2.5. Biofouling assessments

To examine biofouling formation on the membranes, LB Broth (5 g/L) feed solutions were prepared to incubate the bacteria (*E. coli* BL21). Several different experiments were done to examine biofouling formation. The conditions of biofilm formation and analysis are listed in Table 5. Initial bacterial concentration was equal to 0.1 CFU/mL for each set of experiment, and flow rate of Set 1 and Set 2 were equal to 0.35 L/h.

Table 5. Experimental conditions of biofilm formation, and analysis.

Experiment	Conditions	Biofilm formation analysis
1	Non-sterile, exposure in flow at room temperature	Measuring initial and final PWP's of the membranes
2	Non-sterile, exposure in flow at room temperature	SEM imaging of dry membranes
3	Sterile, static test, at 37^{o}C	Gluteraldehyde fixation of the bacteria on the membranes, then SEM imaging of the membranes

CHAPTER 3:

RESULTS AND DISCUSSION

3.1. Chemistry

3.1.1. Modification

Modification of poly(ether sulfone) (PES) (**1**) was done through nitration, reduction and acetylation reactions. Initially nitro groups were installed to obtain PES-NO_2 (**2**), then the nitro groups were reduced to amine groups by reduction reaction to obtain PES-NH_2 (**3**), and amine groups were acetylated to get amide groups of PES-NHAc (**4**). The reaction steps are shown in Figure 16.

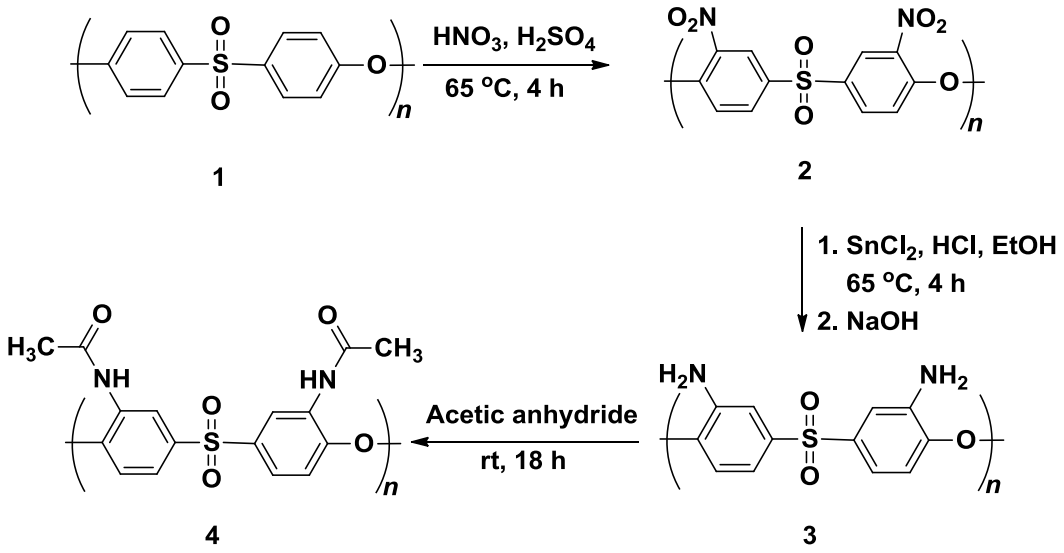

Figure 16. Reaction scheme of nitration, reduction, and acetylation.

3.1.1.1. Nitration of PES

Four different nitration reaction conditions were examined. Reactants and reaction conditions were varied, and PES-NO_2 (**2**) products were obtained.

The procedure **a** was obtained by subjecting the PES to nitration with nitric acid in the presence of sulfuric acid (see Table 2). In the course of the reaction, the polymer first got soft, then brittle. The color of the polymer turned from white to yellow.

The reaction was monitored by FTIR. To observe the difference in the spectrum, pure PES and nitrated PES (PES-NO_2) were analyzed (Figure 17, and Figure 18). The expected peaks for PES were aromatic C-C stretchings between 1500-1400 cm^{-1} and 1600-1585 cm^{-1}. This two regions may shift to low and high fields in the presence of a neighbour electron-donating and electron-withdrawing groups to aromatic structure. FTIR spectrum of PES corralated with this expectation. Two peaks at around 1483 cm^{-1} and 1575 cm^{-1} are arising from aromatic C-C stretching of PES**.** The peak at around 3068 cm^{-1} is arising from C-H stretching. The peak at around 1100 cm^{-1} is arising from ether C-O stretching.

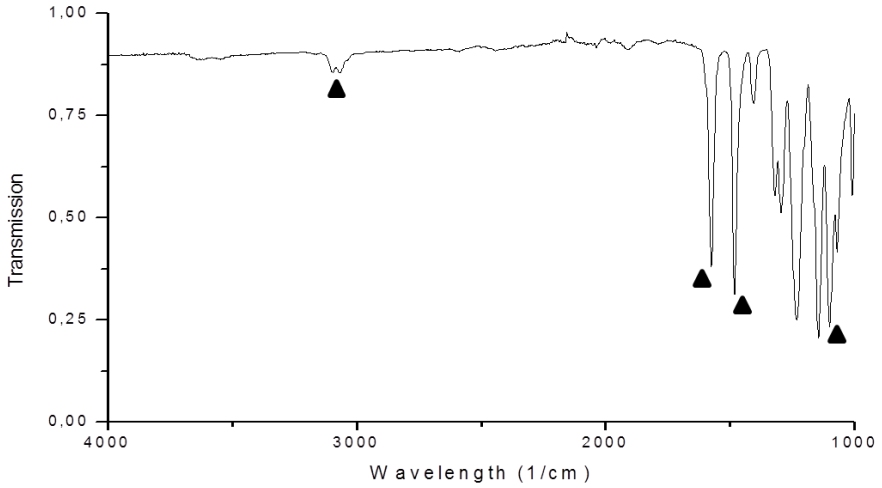

Figure 17. FTIR spectrum of PES (1).
(1100 cm^{-1}, 1483 cm^{-1}, 1575 cm^{-1}, 3068 cm^{-1})

After the nitration reaction of procedure **a**, the product was verified with a peak at around 1535 cm^{-1} appearing on FTIR spectrum. This peak is characteristic of aromatic nitro peaks. It is also observed the ether stretching for PES-NO_2 at around

1100 cm^{-1} is weaker than PES' FTIR spectrum, that indicates the breakage of the backbone occured from ether bonds. ^{1}H NMR was also used for characterization of the compounds dissolving in DMSO-d_6. As seen in Figure 19, the PES ^{1}H NMR spectrum showed two doublets, each accounting for two protons resonate at 7.27 and

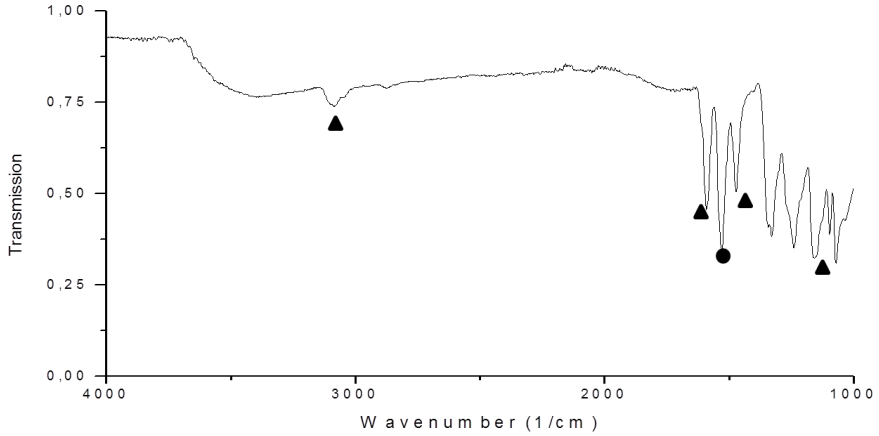

Figure 18. FTIR spectrum of PES-NO_2 (a). (1535 cm^{-1})

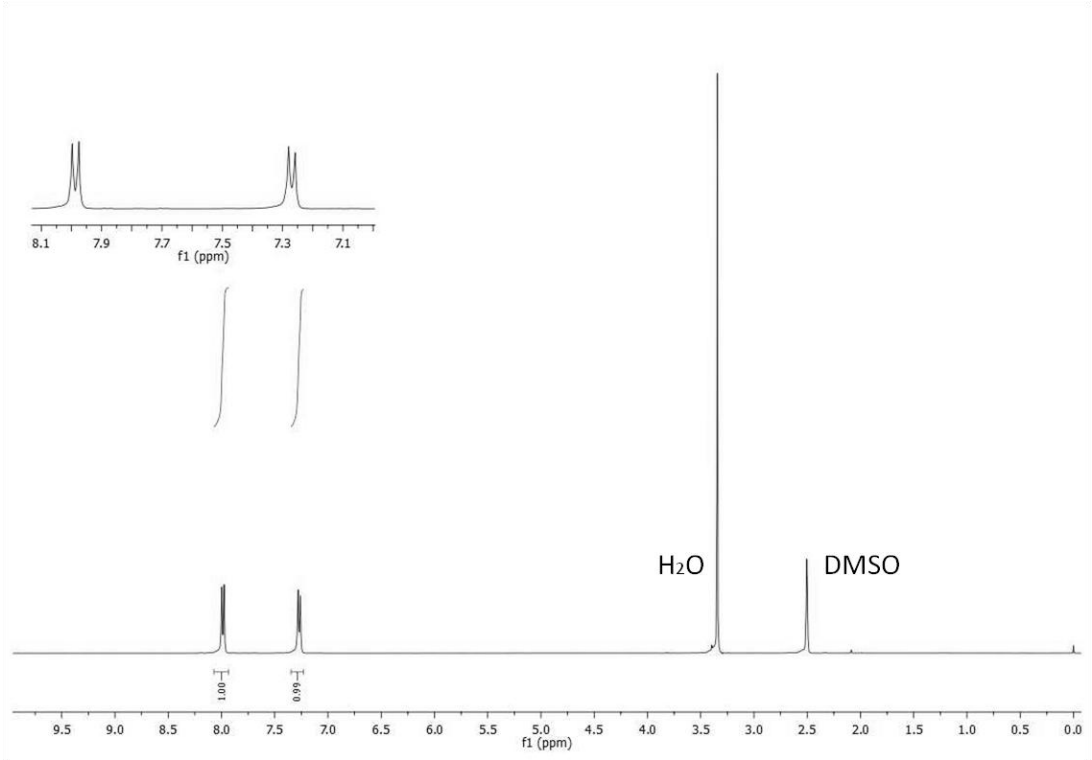

Figure 19. ^{1}H NMR spectrum of PES (1).

8.00 ppm. The PES-NO_2 ^{1}H NMR showed three distinct peak resonating at 7.68, 8.41, and 8.84 ppm (Figure 20). Each of these peaks integrates for one proton, relatively. The peak at 7.68 ppm is a doublet due to the ortho-coupling (J=8.8 Hz). The peak at 8.41 ppm appears as doublet of doublet (J=8.8 Hz, J=2.1 Hz), this arises due to ortho- and meta-couplings. The peak at 8.84 ppm appears as doublet (J=1.9 Hz) due to meta-coupling. From these data, we conclude that the nitrated structure is the one shown in Figure 16. The structure shows that nitration takes place on the carbon which is ortho to oxygen.

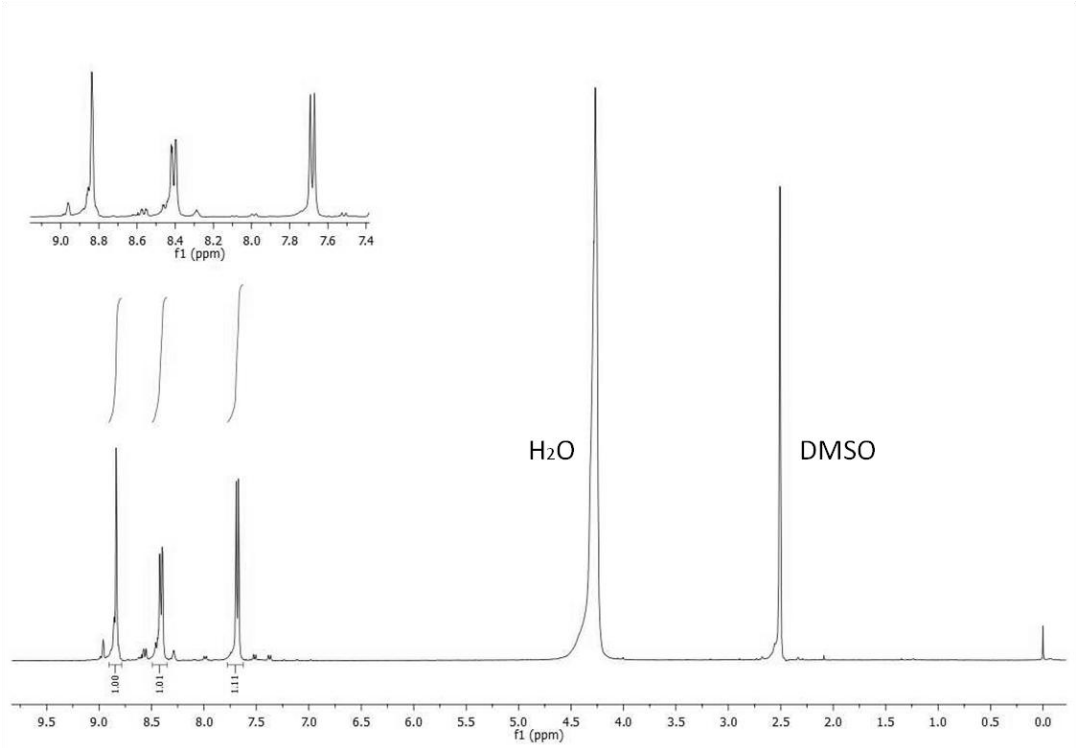

Figure 20. ^{1}H NMR spectrum of PES-NO_2 (a).

Since the breakage of the polymer backbone was obtained fort he procedure **a**, alternative procedures were examined. The procedure **b** was obtained by subjecting PES solution to nitration with ammonium nitrate in the presence of trifluoro acetic anhydride (TFAA) (see Table 2). The characteristic nitro peak at around 1536 cm^{-1}

appeared on FTIR spectrum (see Appendix Part A). Yet, the nitro peak was weaker than aromatic C-C stretching peaks. That indicates the degree of substitution is low. Also, the chemicals needed were not easily accesible, therefore we tended to try other procedures.

The procedure **c** was obtained by dissolving PES in nitrobenzene. The solution was subjected to nitric acid and sulfuric acid for nitration. Collection of a few part of the product was analyzed by FTIR, however characteristic nitro peak was not seen on the spectrum.

The procedure **d** was obtained by subjecting PES solution to nitric acid and sulfuric acid for nitration. The product was characterized by ATR FTIR spectrometer. The characteristic nitro peak appeared at around 1528 cm^{-1} (see Appendix Part A). The nitration reaction efficiency of dissolved PES was examined with procedure. Although nitration was observed, since the removal of the solvent was not easy, the procedure was not preferred.

With all the results of experiments, even though a decrease in molecular weight was observed upon nitration of PES with procedure **a**, the other nitration procedures were not efficient enough. Therefore, we continued with procedure **a** thought this thesis.

3.1.1.2. Reduction Reactions

Three different reduction reaction conditions were examined. Reactants and reaction conditions were varied, and PES-NH_2 (**3**) products were obtained.

The procedure **a** was obtained by reducing PES-NO_2 to PES-NH_2 with the presence of $SnCl_2$, HCl, and EtOH as a solvent. The color of the polymer turned to brown after the reduction. The reaction was monitored by FTIR which showed the disappearance of peak at around 1535 cm^{-1} and appearance of a weak and broad peak at around 3350 cm^{-1} (Figure 21). Amine obtained from the reaction, was in salt form. Therefore, the product was made alkaline with NaOH. Although we observed reduction reaction of nitro group to amino, not all nitro groups were reduced to amino groups. Therefore, the nitro peak still appeared on FTIR spectrum of PES-NH_2. The PES-NH_2 ^1H NMR showed four distinct peaks resonating at 5.57, 6.80, 6.99, and 7.27 ppm (Figure 22). When we superimposed the spectra of PES-NO_2 and

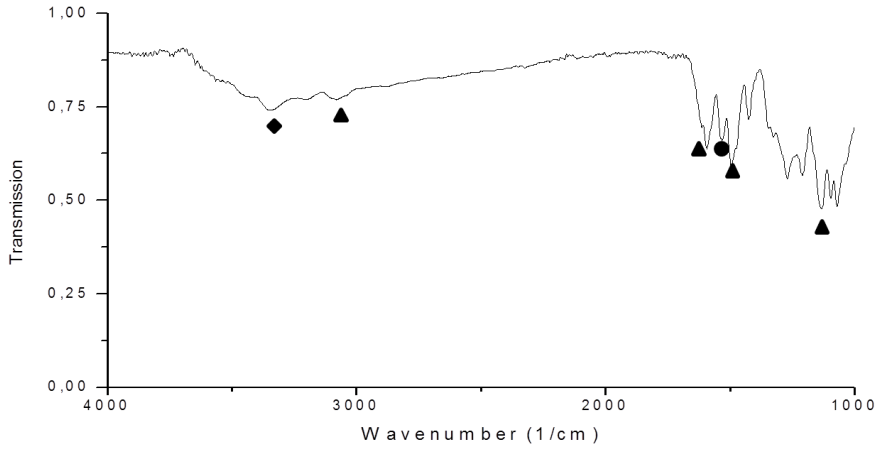

Figure 21. FTIR spectrum of PES-NH_2 (a). (3350 cm^{-1})

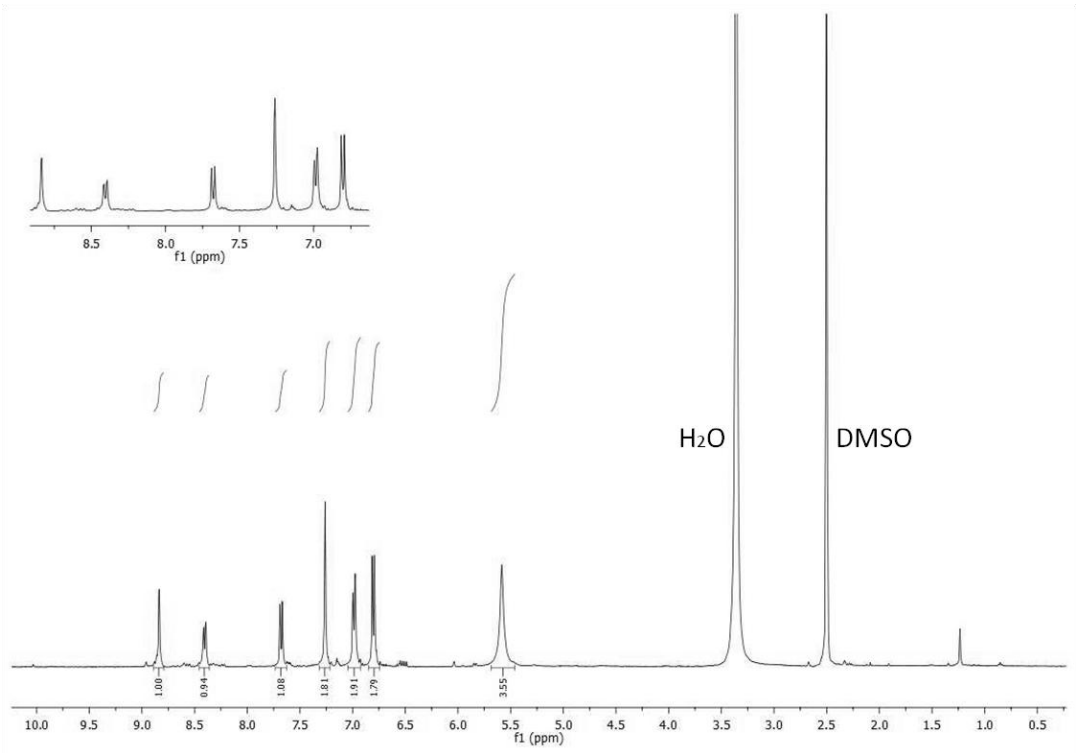

Figure 22. NMR spectrum of PES-NH_2 (a).

PES-NH_2, it was observed that nitro bonded aromatic ring protons were still present in the product. The peak at 5.57 ppm is a singlet, which arises from –NH_2 group integrated for two protons. The peaks at 6.80 is a doublet due to ortho-coupling

(J=8.4 Hz), at 6.99 ppm is a doublet of doublet due to ortho- and meta-couplings (J=8.2, J=2.0 Hz), 7.27 ppm is a doublet due to meta-coupling (J=1.9 Hz).

The intergation of each peak due to the unreacted nitro groups (see Figure 20 to compare with Figure 22) are set to one, the integration of new peaks due to the reduced ones (PES-NH_2) are proportionate to two. Therefore, 67% of the nitro groups are reduced. These peaks shifted to high field relative to peaks of PES-NO_2 due to the fact that amine is an electron donating group, whereas nitro is an electron withdrawing group.

To end up with complete reduction ratio, alternative procedures were examined. The procedure **b** was obtained in the presence of phenylhydrazine. The product was monitored by FTIR which showed appearance of a weak and broad peak at around 3350 cm^{-1}. However, characteristic PES peaks in the range 1400-1500 cm^{-1} were disturbed after the reaction (see Appendix Part A). Also, a new peak appeared at around 1590 cm^{-1}, which may be because of the residual phenylhdrazine. Since the reaction was not efficient, and the chemical used was extremely hazardous, we decided not to proceed with this procedure.

The procedure **c** was obtained by hydrogenation reaction. High pressure and temperature conditions were used for hydrogenation. Yet, eventhough the reduction was done, we could not collect the product. During the separation of Pd/C catalyst, the polymer could not be collected.

Procedure **a** provided the highest reduction yield, this procedure has been employed throughout this thesis.

3.1.1.3.Acetylation reactions

Three different acetylation reaction conditions were examined. Reactants and reaction conditions were varied, and PES amide (PES-NHAc) (**4**) products were obtained.

The procedure **a** was obtained by treating PES-NH_2 with acetic anhydride to PES-NHAc after 18 h of stirring. The reaction product was also initially characterized by FTIR (Figure 23). The peak at around 1673 cm^{-1} indicates the amide formation. The

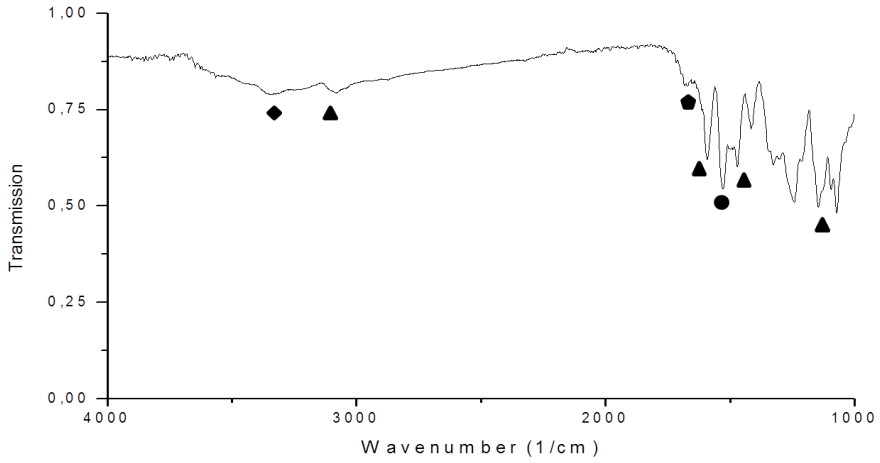

Figure 23. FTIR spectrum of PES-NHAc (a). (1673 cm^{-1})

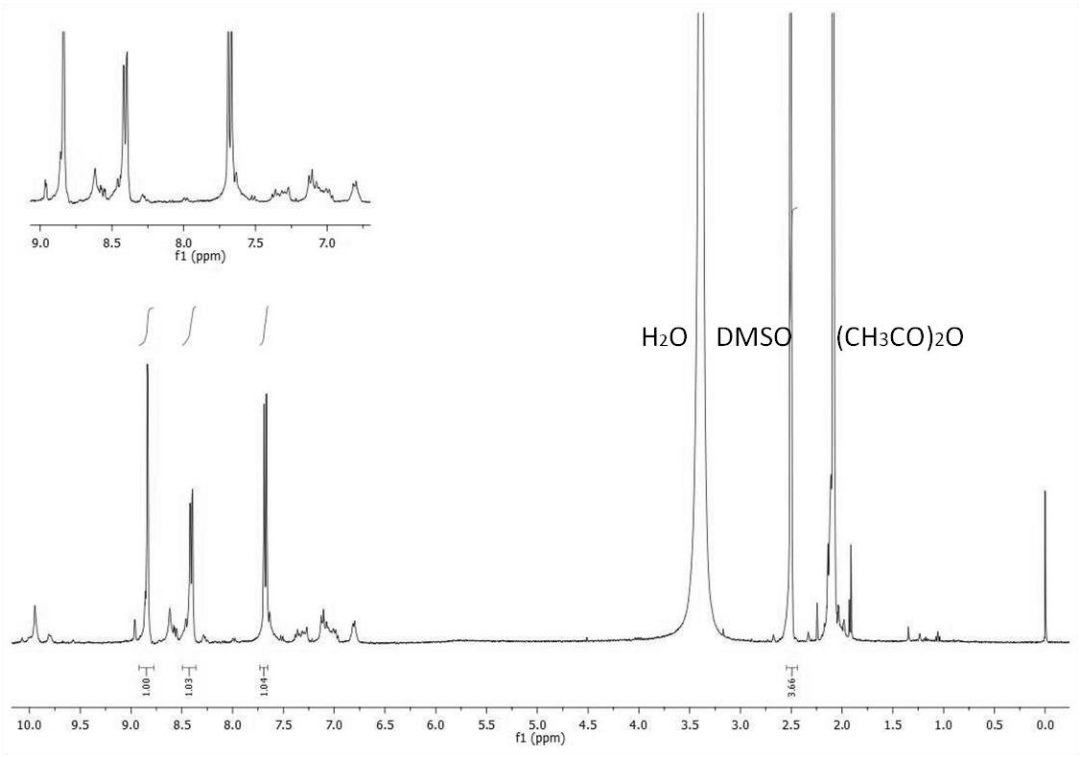

Figure 24. NMR spectrum of PES-NHAc (a).

peak resulting from N-H stretching at around 3300 cm^{-1} got smoother after the acetylation. The color of the polymer turned to light brown. ^{1}H NMR spectrum of PES-NHAc showed a peak at 2.1 ppm which is due to the $–CH_3$ of acetylamide

(Figure 24). Even though we wanted to assign the ^{1}H NMR spectrum of PES-NHAc peak by peak, it was not possible to do so because of the broadening in the aromatic region. This broadening arises due to the conformational and lack of full acetylation**.** Neverthless, we characterized this compound by combining FTIR and ^{1}H NMR spectrum.

To obtain high acetylation, we examined alternative reaction procedures. The procedure **b** was obtained by following procedure. The PES-NH_2 was treated with sodium acetate in the presence of HCl and water to yield PES-NHAc after 12 h of stirring at 0^oC to room temperaure. The reaction product was characterized by FTIR. The peak at around 1682 cm^{-1} indicates the amide formation (see Appendix Part A). The peak resulting from N-H stretching at around 3300 cm^{-1} was still present. Since the carbonyl peak was quite weak, we decided to examine another procedure.

The procedure **c** was examined in order to increase the efficiency of procedure **a.** The polymer was dissolved in DMF. Triethylamine was added to make the solution alkaline. After the reaction the product was precipitated in water, washed with water and then ethanol, then dried. The reaction product was characterized by FTIR. The peak at around 1771 cm^{-1} indicates the presence of carbonyl group (see Appendix Part A). This amide peak was later assigned to acetic anhydride, which was the reactant. Furthermore, it is hard to separate the solvent totally from the product, which was going to be a source of uncertainity during the preparation of the membranes. Therefore, we proceed with the procedure without any solvent.

3.2. Membrane

3.2.1. Membrane preparation

During the preparation of the membranes, several dope solutions were examined. The results are summerized in Table 6.

Initially, the dope solutions were prepared as 10 wt % polymer (PES, PES-NO_2, PES-NH_2, and PES-NHAc) in NMP. Between those polymer solutions, only PES membrane could be prepared by phase inversion method. Modified polymer solutions dispersed in water bath after coagulation. This may be because of several reasons. One of them is the polymer molecular weight and/or polymer concentration

Table 6. Membrane dope solution contents and observations.

Solutions	Observations
10 wt % PES in NMP	Membrane formed
10 wt % PES-NO_2, PES-NH_2, and PES-NHAc in NMP	Dispersed polymers in coagulant
15 and 20 wt % PES-NO_2 in NMP	Dispersed polymers in coagulant
6, 8, 10, 15 wt % PES-NO_2 blended with 10 wt % in NMP	Membranes formed. Fragility increased with increasing PES-NO_2

being insufficient to get polymer-lean phase nuclei to grow within a polymer rich phase. To examine that, membranes were tried to be prepared with 15 wt % and 20 wt % PES-NO_2 and PES-NH_2 solutions. Yet, the polymers still coagulated as dispersions in the water. Obtaining PES membrane, but not modified PES membranes indicated that a breakage in the backbone might have occured during the modification reactions. The viscosities of the solutions in equal concentration give information about the molecular weight of polymers. The viscosities of the polymers in DMF were measured by Ubbelohde cappillary viscometer. The calculated intinsic viscosity of PES solution was 0.6 dL/g, whereas the intrinsic viscosities of PES-NO_2, PES-NH_2 and PES-NHAc were around 0.2 dL/g (see Appendix Part E). From these measurements, it could be concluded that the nitration reaction step caused a lowering in the molecular weight, whereas the rest of the reactions did not. In order to determine the molecular weights of the polymer, we intented to make gel permeation chromatography (GPC). However, the polymers were not soluble in tetrahydrofuran (THF), which is widely used solvent of GPC instrument. Therefore, we solved the dispersion problem by preparing blends of polymers. We prepared membranes from 6, 8, 10, and 15 % PES-NO_2 blending with 10 % PES solutions dissolving in NMP. We observed that increasing PES-NO_2 either increases dispersion and membrane could not be achieved, or increases the fragility of the membrane. Therefore, we decided to proceed with the blends of 6 wt % modified PES and 10 wt % PES solutions.

Finding of the proportions of the polymers, we observed low solubility of PES-NHAc in NMP, which was the first solvent tried. To choose a standart solvent for all our modified and pristine PES polymers, we dissolved PES-NHAc in NMP, DMF, DMAc, and DMSO under same conditions and proportions. They demonstrated similar solvation behaviour since their solubility parameters are close to each other. Yet, the solution prepared with DMF was observed to be more homogenuous. Therefore, DMF was used as the solvent for the rest of the study.

During the phase inversion of the polymer solution, the coagulant medium became dirty with the color of modified polymer. Depending on that observation, we concluded the polymer ratio in the membrane was not equal to one in the dope solution's. In order to determine PES/modified-PES ratio, ^{1}H NMR analysis of membranes were done. The spectrum of PES/PES-NHAc membrane was not clear to calculate the ratio, on the other hand it is calculated the PES/PES-NH_2 ratio is 10 to 4 (see Appendix F).

3.2.2. Membrane chlorination and chlorine release assessments

As shown in Figure 25, chlorination and chlorine release are in an equilibrium in aquous medium.

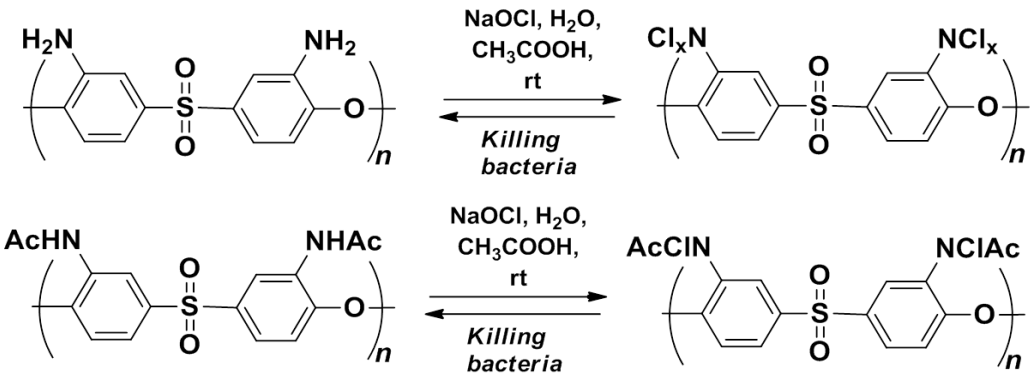

Figure 25. Reaction scheme of chlorination PES-NH_2 and PES-NHAc polymers.

3.2.2.1. Chlorination

In the initial stages of our study, we chlorinated the membranes for 3 hours with undiluted NaOCl solution, which is including 15 % active chlorine. The pH was

brought to 7 with acetic acid, and we got HOCl solution. However, we observed that the chlorinated membranes got fragile. Since sufficient mechanical strength of the membrane is necessary to operate the membrane under pressure, we examined five different chlorine concentrations; 0.3, 1, 5, 10, and 15 % active chlorine; and three different chlorination times; 10, 60, and 120 min, for chlorinating the membranes. Three membranes were examined for each measurement, average values are used in graph and standart deviations are labelled on bars.

Figure 26 and Figure 27 show the contact time of membranes to HOCl solutions. When the effect of feed solution concentrations were analyzed, it was observed the loaded chlorine amount increase with increasing solution chlorine concentration. When we look at the difference in contact time sets, it was observed that there is no significant difference between 10 min and 60 min contact time. However, chlorine amount was gradually decreases in 120 min, and increasing chlorine percent increased the chlorine loaded. This is because the chlorine is in equilibrium; initially chlorination is forward reaction, then chlorine of the feed solution decomposes to Cl_2 and evaporates in time, therefore loaded chlorine is released back to the solution. Consequently, the chlorine loaded in 2 hours is less than in 10 minutes. In conclusion, we chose 10 min contact time with 5% chlorine including feed solution for both type of the membranes.

We aimed to find an optimum chlorine concentration in the solution, and chlorination time. Even though the highest chlorine concentration yields the highest chlorine, since it makes membrane more fragile we chose 5% active chlorine concentration for use in this study. For the time preference, a short chlorination time was the preferable in the first place. The results of 10-minute and 60-minute chlorination assessments showed similar behaviour, whereas 120-minute chlorination was less effective. Therefore we concluded 10-minute chlorination is the most efficient between three of the spans.

In conclusion, HOCl solution containing 5% active chlorine was used for chlorination for 10 min.

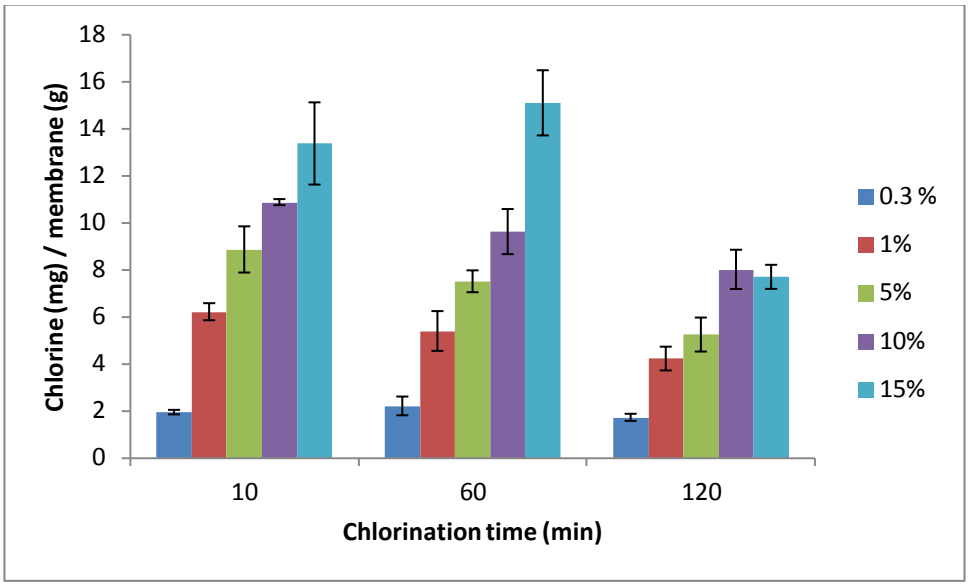

Figure 26. Chlorination of PES/PES-NH_2 membrane.

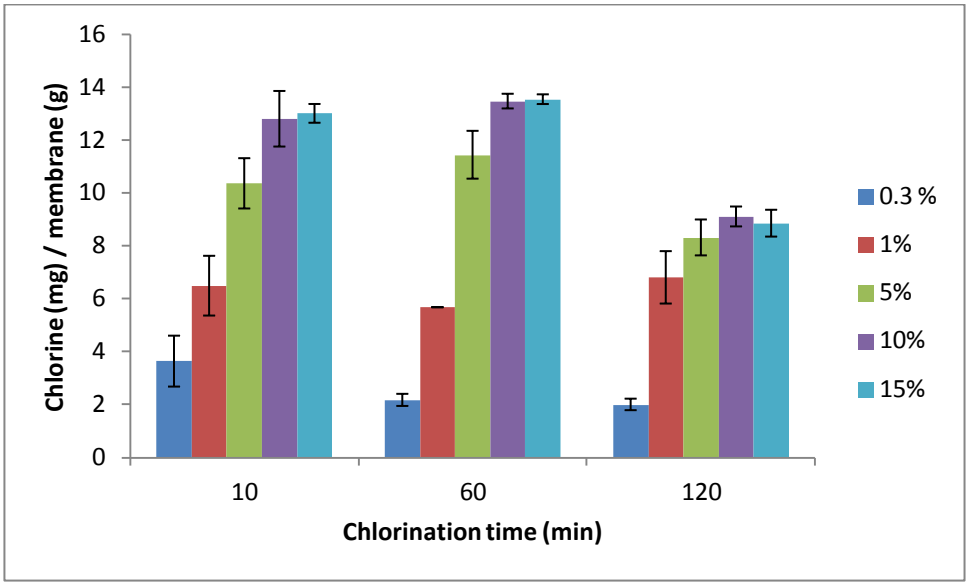

Figure 27. Chlorination of PES/PES-NHAc membrane.

Percent chlorination per hydrogen, that can undergo chlorination, is calculated as about 7 % for PES/PES-NH_2 membrane, and about 12 % for PES/PES-NHAc membrane for 10 minutes chlorination with 5% solution. See Appendix Part B for the details of the calculation.

3.2.2.2. Chlorine release

In order to predict the effective biocidal time of the chlorinated membranes, initially chlorine release to ultra pure water was examined. Membrane coupons with same

area were weighted, then chlorinated for 10 min in HOCl solution containing 5% active chlorine. The chlorinated membranes were gently washed with ultra pure water to remove adsorbed chlorine on the surface.

The membrane coupons were placed in cross-flow system for providing continuous fresh ultra pure water flow. Once in a while, a coupon was taken out, and the amount of chlorine charged was determined by iodometric titration. Three membranes were examined for each measurement, average values are used in graph and standart deviations are labed on Figure 28 and Figure 29.

As shown in Figure 28, PES/PES-NCl_2 membranes release all the chlorine in around 7 hours, whereas PES/PES-NClAc membrane keeps chlorine for longer time in water. For the PES/PES-NClAc membrane, the experiment was carried out for 23 hours. It was observed the chlorine released very slowly, and after 23 hours the membrane still had chlorine.

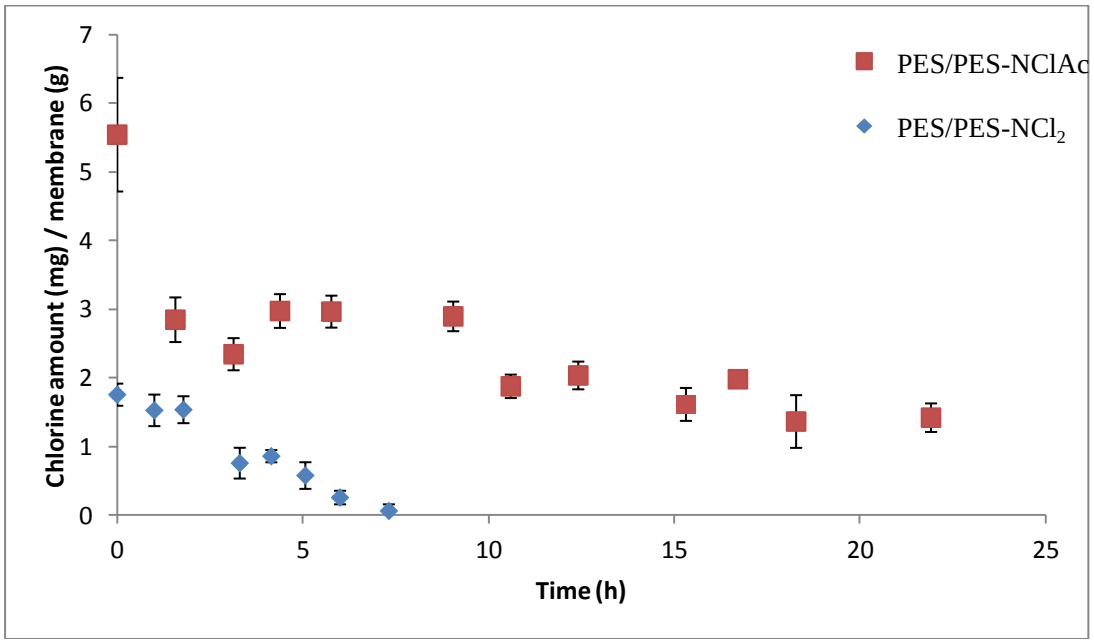

Figure 28. Chlorine release in pure water

Based on the initial experiment, we concluded that PES/PES-NClAc membrane may be more effective for antibiofouling purposes. Therefore, we carried out chlorine release in bacterial medium for only PES/PES-NClAc membrane.

E. coli BL21 was inoculated in LB Broth (5g/L) liquid nutrient. 10^5 CFU/mL and 10^8 CFU/mL bacterial solutions were prepared. PES/PES-NHAc membrane coupons with same area were prepared, weighed and chlorinated in 5% HOCl solution, which was neutralized by acetic acid. The chlorinated membranes were exposed to continuous flow of bacterial solution. Once in a while three membranes were taken, and the amount of the chlorine charged was determined by iodometric titration.

The results of the chlorine release assessements are shown in Figure 29. It was observed that higher concentration of bacteria consumes the chlorine more rapidly than lower concentration of bacterial solution. This indicates chlorine is consumed faster with the bacteria or any other oxidizable species, as expected.

Another experiment was done with PES/PES-NClAc membranes chlorinated with 15% HOCl solution, which is the non-diluted concentration. The membranes were damaged from the non-diluted HOCl solution, and lost their mechanical strenghts. However, they were charged with more chlorine with that solution. Since we observed that chlorination in 5% HOCl solution releases the chlorine in a few hours in the presence of oxidizable species, which may not be very efficient to prevent biofilm formation, we wanted to see whether membranes loaded with higher chlorine concentration can be more effective in slowly releasing chlorine. In conclusion, increasing chlorine amount on membrane and decreasing bacterial solution increases effective antimicrobial time during the filtration.

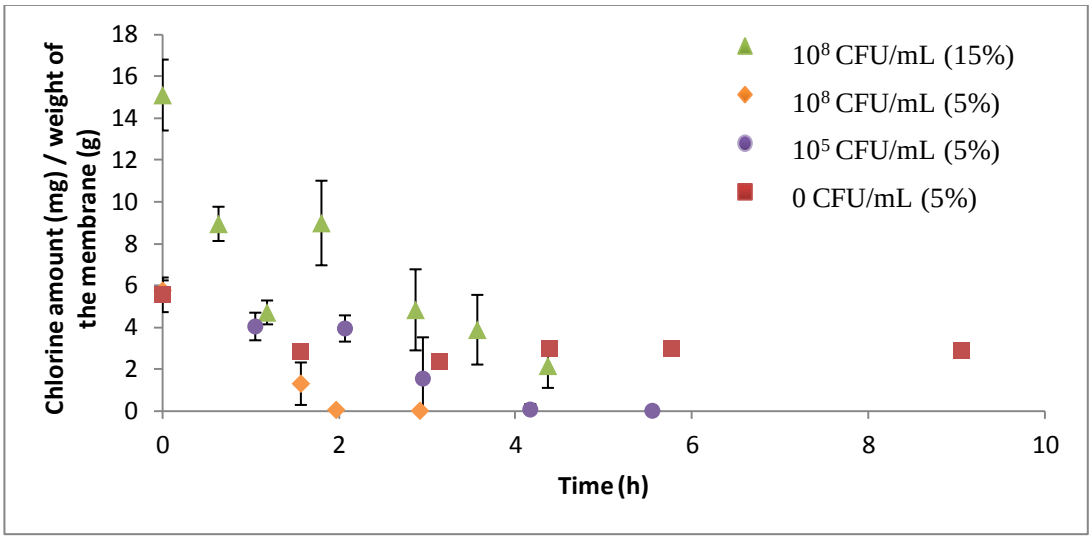

Figure 29. Chlorine release of PES/PES-NClAc membrane to *E.coli* solution.

3.2.3. Membrane characterization

3.2.3.1. SEM

The surfaces and cross-sections of the membranes were monitored by SEM (Figure 30). Microporous skin with macroporous support, and macrovoids were observed for each membrane. The morphology of a membrane is related with polymer-solvent-nonsolvent interactions, that causes difference in thickness and pore sizes of the membranes. The membrane thicknesses were measured by ImageJ software**.** The cross-sectional thickness of the membranes prepared from 16 wt % polymer dope solutions were higher than the membrane of 10 wt % PES solution. Casting the dope solution with 250 μm thickness, 16% solution includes more polymer.

Although 10% solution leads higher macrovoid volume, in total, higher polymer concentration resulted in a thicker membrane. Furthermore, the thickness increases in the order PES (10 wt%) < PES (16 wt%) < PES/PES-NH_2 ~ PES/PES-NCl_2 < PES/PES-NHAc ~ PES/PES-NClAc membranes. This difference possibly arises from the polymer-solvent-nonsolvent interactions. Modified polymers include N-H, N-O, N=O groups in the structure, which give a more hydrophilic behaviour to the polymer. When the non-solvent is water, it is known from the literature that the membrane morphology may be greatly altered with increasing hydrophilicity of the coagulating polymer [37, 38]. On the other hand, the chlorinated forms of the membranes gave similar measurements with non-chlorinated forms. This shows the chlorination which is done after membrane fabrication does not affect the membrane morphology, as expected.

It is seen that 10% PES solution gave the largest pores in the skin layer. This is because at a low polymer concentration, phase inversion within the two-phase region results in a lower ratio of polymer rich phase to polymer-lean phase [1].

3.2.3.2. Contact angle measurement

The hydrophilic/hydrophobic character of the membranes affect the adsorption of the bacteria to the surface. In order to determine the hydrophilic/hydrophobic character of the membrane surface, contact angle measurement was done on the membranes.

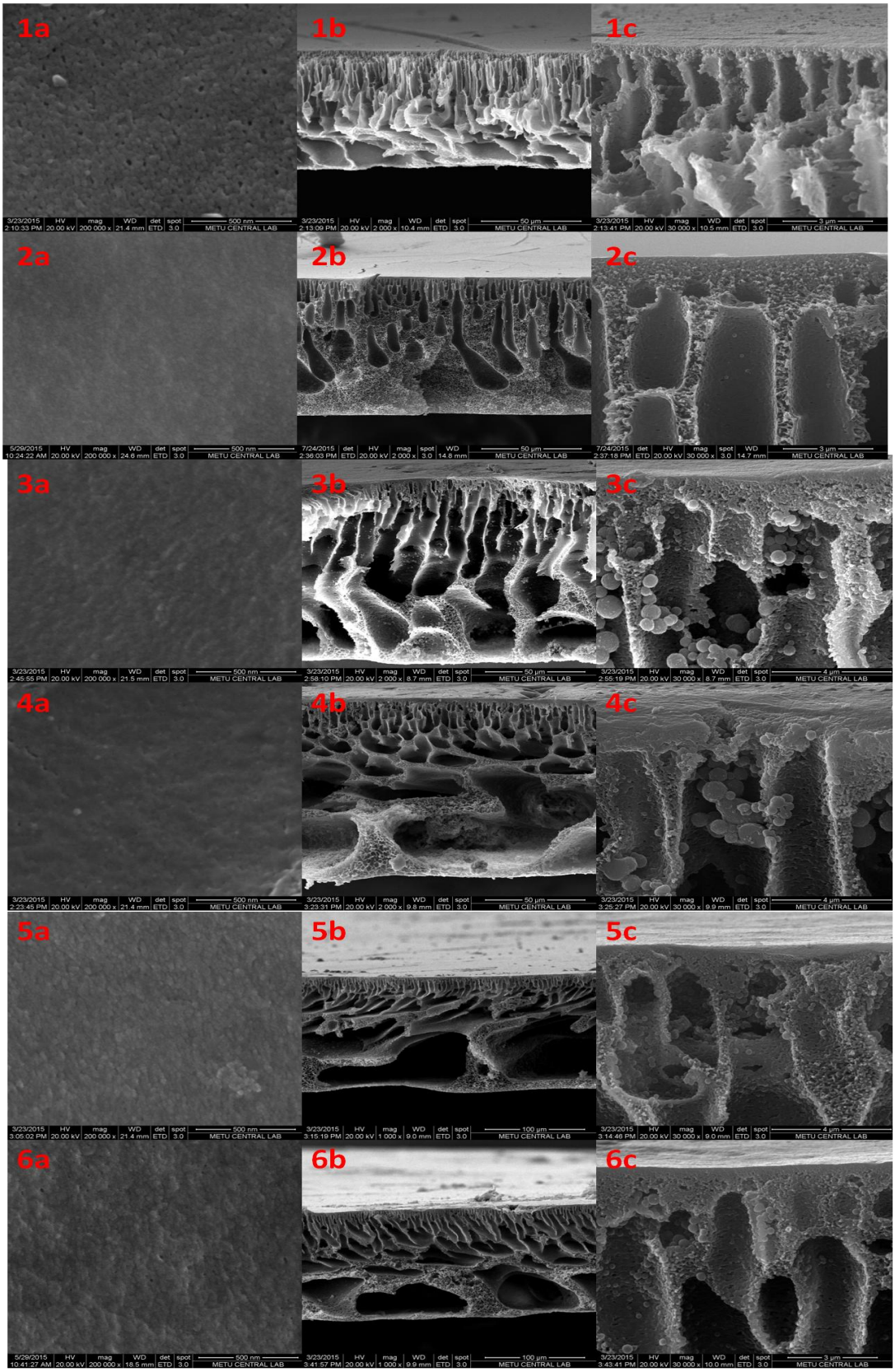

Figure 30. SEM images of 1) PES 10%, 2) PES 16%, 3) PES/PES-NH_2, 4) PES/PES-NCl_2, 5) PES/PES-NHAc, and 6) PES/PES-NClAc membranes of a) surface, b) entire cross-section, and c) skin layer cross-section.

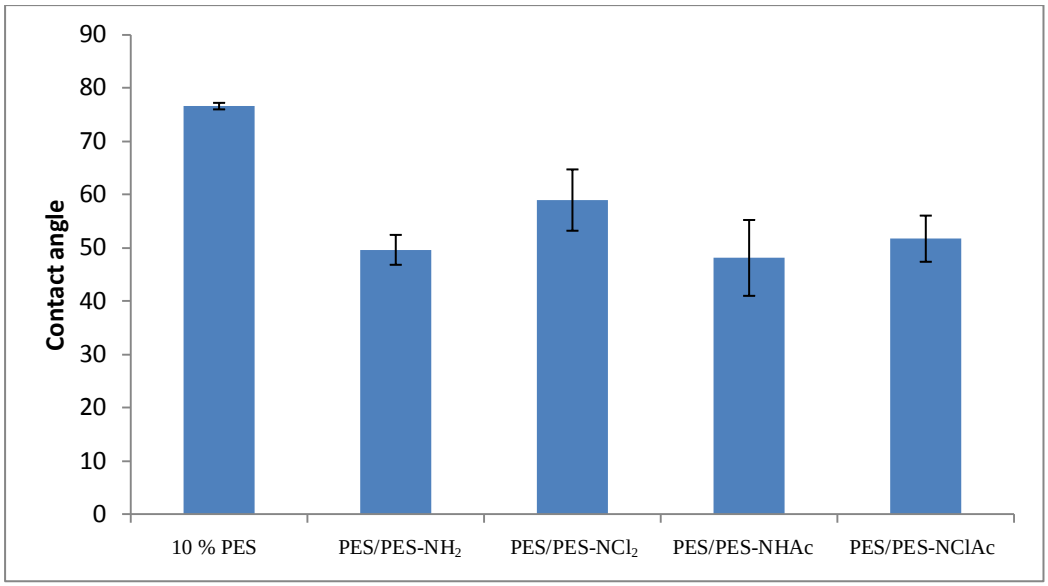

Figure 31. Contact angles of the membranes.

The average value of the contact angles measured from at least 10 different points of the membranes are shown in Figure 31. It is shown that pure PES membrane is more hydrophobic than modified membranes. Modified membranes show similar hydrophilic behaviour. All in all, the contact angle of all membranes are less than 90^{o}, therefore the PES and PES based modified polymers can be classified as hydrophilic.

3.2.3.3. Membrane performance assessments

Pure water permeance (PWP) of membranes are shown in Figure 32. It was observed that PES membrane made from 10% PES solution has highest permeance, and

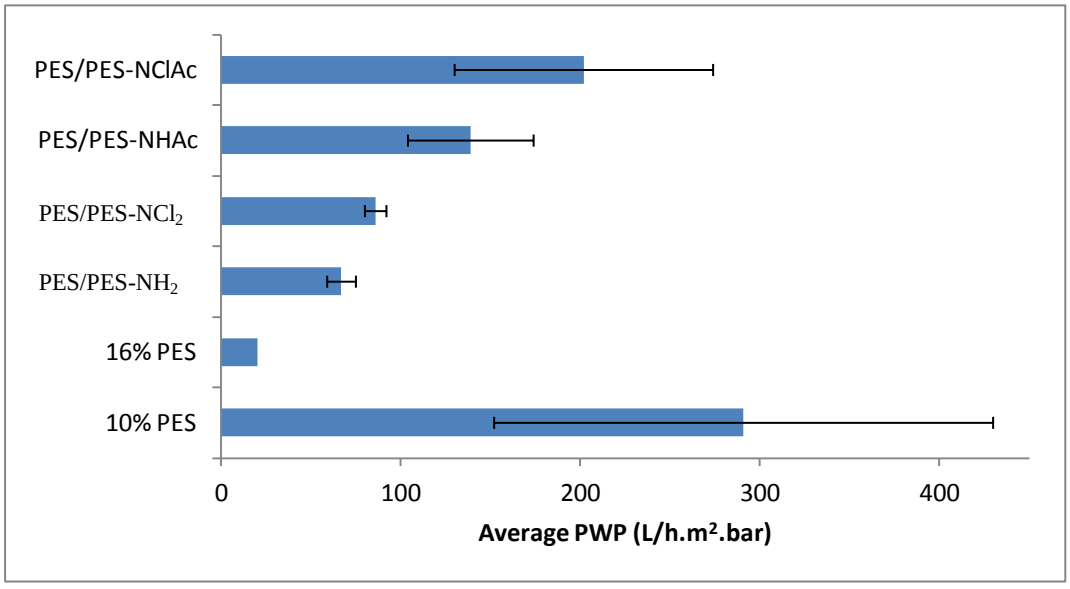

Figure 32. Pure water permeances (PWP) of the membranes.

chlorinated and non-chlorinated forms of modified membranes show similar permeance. Permeance is affected by pore size, porosity, and skin layer thickness. Pure 10 % PES membrane shows a high deviation in permeances. It may because it has a very thin skin layer which can be heterogenuous throughout the membrane surface and between different samples. Pore size of 16% PES membrane is lower and skin layer (which may be roughly defined as the thickness until the macrovoids, where the most of the resistance to flow occurs) thickness of 16% PES membrane is higher than 10% PES membrane, which causes lowering in the permeance. Modified membranes has lower polymer content than 16 %, due to the loss during the phase inversion. Since the molecular weight of modified polymers are less than PES, as mentioned in Section 3.2.1., the membrane composition include less modified polymer than 6 %.

Permeances of chlorinated and non-chlorinated forms of modified membranes show similar behaviour with small difference, as expected. Since chlorination does not affect the morphologies of the membranes, pure water permeances are expected to be similar.

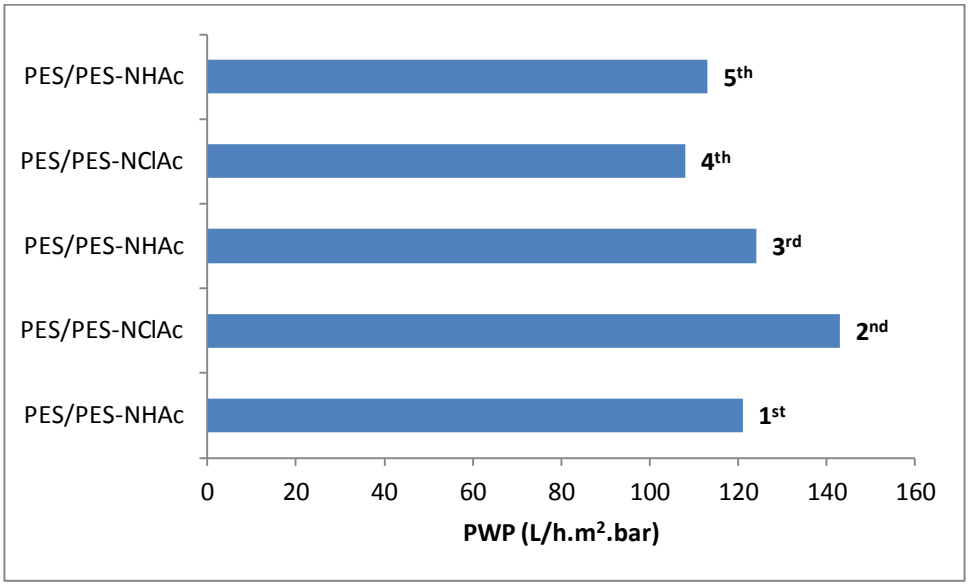

Figure 33. Pure water permeances of PES/PES-NHAc and PES/PES-NClAc in recycle chlorination and dechlorination.

In order to analyze the effect of chlorination on PWP of PES/PES-NHAc membrane, PWP of a PES/PES-NHAc membrane was measured in a recycle. Initially, PWP of a PES/PES-NHAc membrane was measured, then the membrane was taken out from

the module and chlorinated by 5% HOCl solution. Second PWP measurement was done on this PES/PES-NClAc membrane. afterwards, the chlorinated membrane was taken out and dechlorinated by sodium thiosulfate ($Na_2S_2O_3$). The third PWP measurement was done on this PES/PES-NHAc membrane. The fourth and fifth measurement was repeated with the same procedure. PWPs of PES/PES-NHAc and PES/PES-NClAc measurements are shown in Figure 33**.** It can be concluded that the PWP of membrane is not altered by successive chlorinations.

3.3. Biological assessments

3.3.1. Biocidal assessments

3.3.1.1. Static biocidal assessment

Biocidal activity of the membranes were examined first in static tests. 10^7 CFU/mL bacteria were inoculated on LB Agar (35 g/L), then incubated at 37^oC for 24 h. The growth by bacteria are shown in Figure 34.

PES, PES/PES-NH_2, and PES/PES-NHAc membranes showed similar growth with empty control group, whereas PES/PES-NCl_2 and PES/PES-NClAc membranes generated inhibition zones. This indicates the chlorine is responsible agent from antimicrobial activity, and the modified polymer is ineffective for this purpose.

For the assessment done on *E. coli* BL21, it was observed that the inhibition distance from PES/PES-NCl_2 membrane is 2 cm, whereas the inhibition distance from PES/PES-NClAc membrane is 0.7 cm. In the assessment done on *Bacillus subtilis,* the inhibition distance from PES/PES-NCl_2 membrane is 2.6 cm, whereas the inhibition distance from PES/PES-NClAc membrane is 1.9 cm.

It is shown in Figure 34 that PES/PES-NCl_2 membrane inhibited more area than PES/PES-NHAc membrane. This result is consistent with chlorine release asssessment. Since the PES/PES-NCl_2 membrane releases the chlorine easier, it affects a larger area. Furthermore, PES/PES-NClAc membrane showed less inhibition zone on *E. coli* BL21 than on *Bacillus subtilis*. This is because *E. coli* is a Gram-negative bacterium, which has an outer cell membrane makes it strong organism against biocidal agents, whereas *Bacillus* is Gram-positive, with no outer cell membrane so it is weaker against biocidal agents.

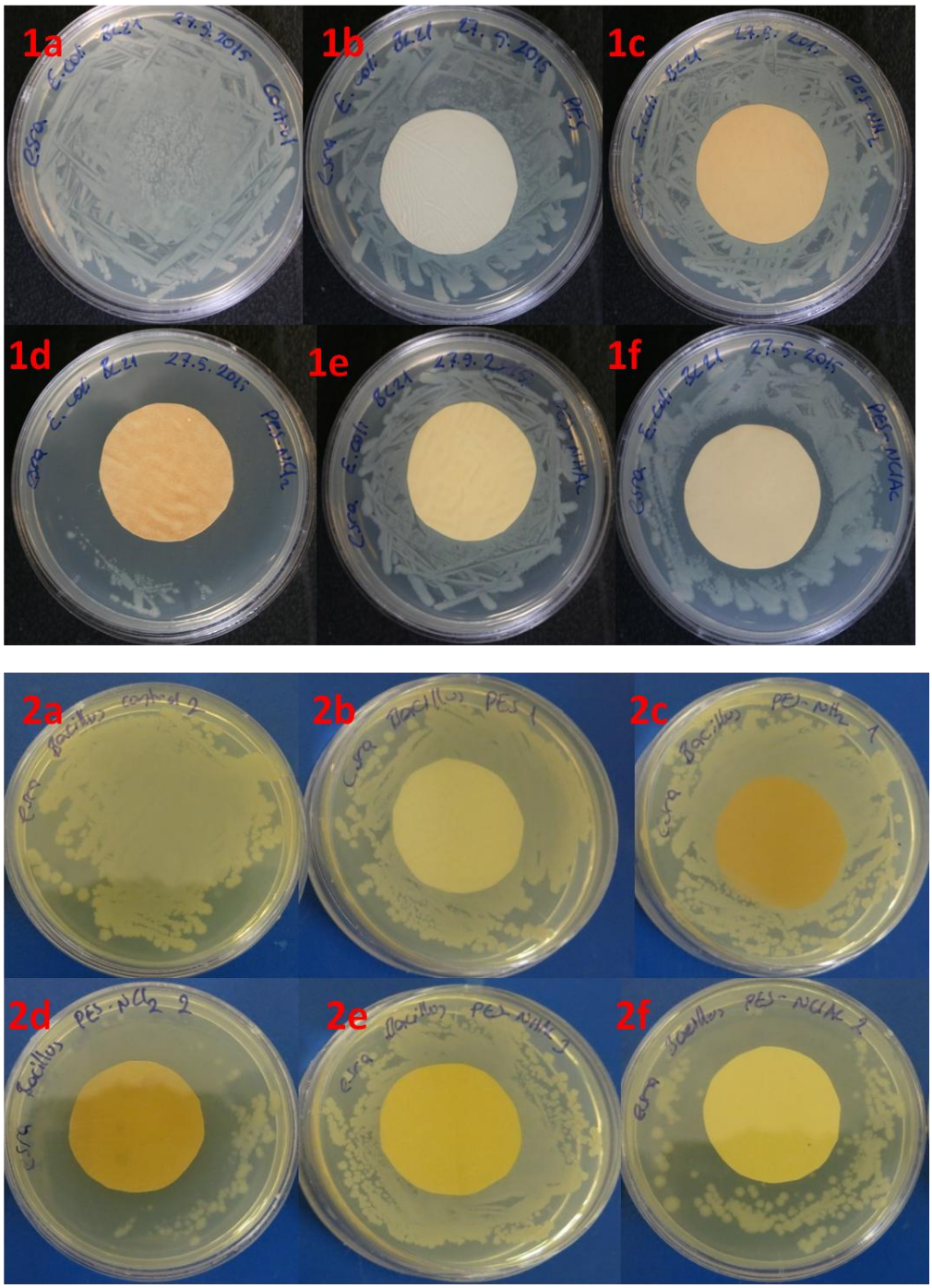

Figure 34. The results of antimicrobial activity assessments. 1) *E. coli* BL21, 2) *Bacillus subtilis*. a) Empty control, b) PES, c) PES/PES-NH_2, d) PES/PES-NCl_2, e) PES/PES-NHAc, and f) PES/PES-NClAc membranes.

3.3.1.2.Kinetic biocidal assessment

To examine the logarithmic reduction of bacterial concentration in an aquous medium in the presence of membranes, a kinetic biocidal assessment was carried out. The initial concentrations of the *E. coli* BL21 solution was 10^9 CFU/mL, which was measured with UV-Vis spectrometry. The stock bacterial solution was diluted to 10^5

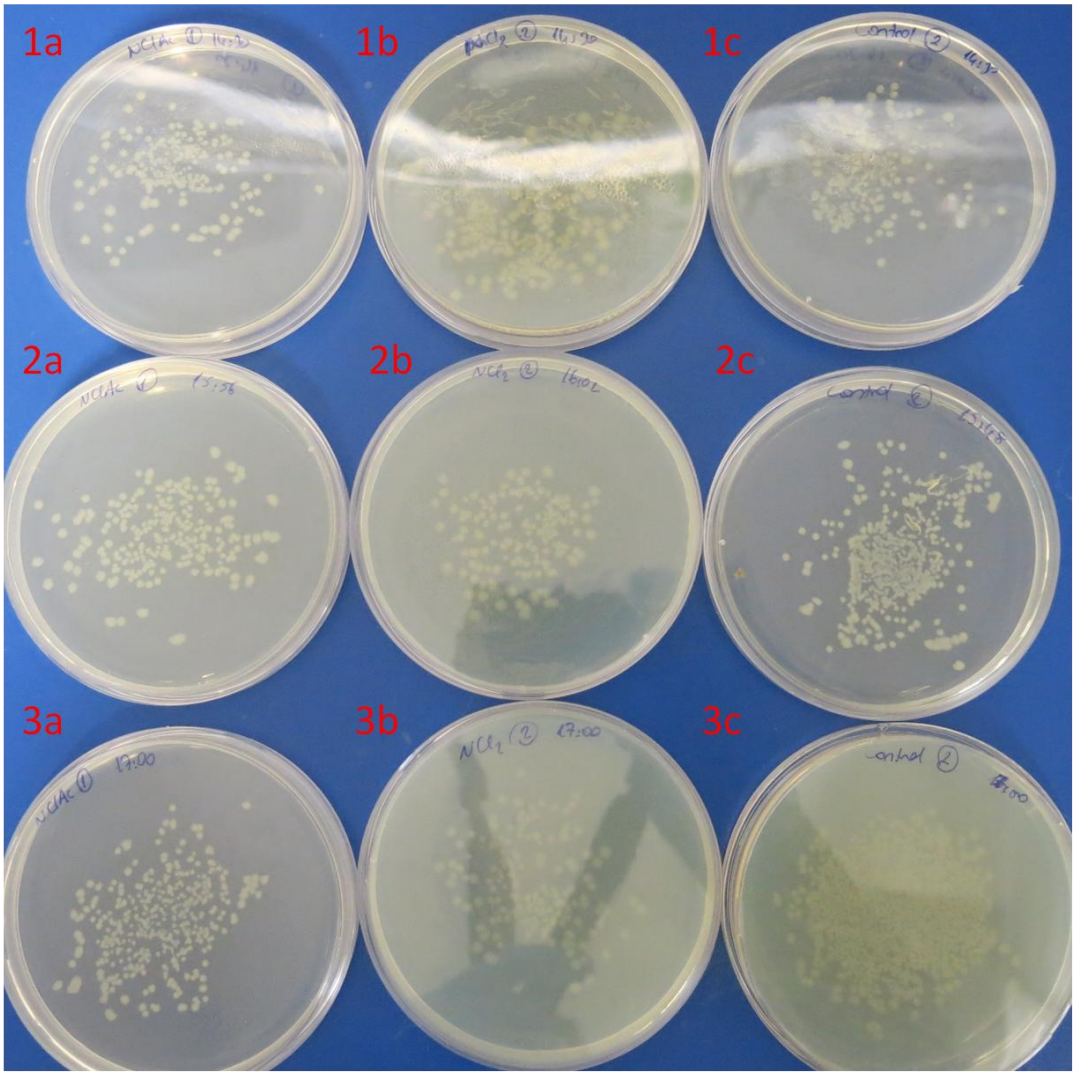

Figure 35. Kinetic biocidal assessment on *E. coli* BL21. a) PES/PES-NClAc exposed, b) PES/PES-NCl_2 membrane exposed, and c) empty control sets of 1) zeroth time, 2) 1.5 h after exposure, and 3) 3 h after exposure.

CFU/mL. The stock solution was divided into six sterile flasks. Two of them were empty control groups, two of them were including PES/PES-NCl_2 membranes, and last two flasks were including PES/PES-NClAc membranes. 20 µL of bacterial solution was collected from each flask at 0, 1.5 and 3 h intervals and inocu lated into

solid nutrient media. The inoculums were incubated at 37°C for 24 h to count the colonies grown. The results are shown in Figure 35, and the number of colonies are listed in Table 7.

Table 7. The counted colony numbers of the results shown in Figure 35.

	Colony number counted		
Time (h)	Control	PES/PES-NCl2	PES/PES-NClAc
0	52	177	177
1,5	663	152	140
3	uncountable	149	237

It is seen that the colony number of control set increases in time. However, sets where biocidal membrane coupons were placed showed similar colony numbers. This indicates the chlorine hinders the reproduction of the bacteria, yet it is inefficient to kill all, for the given starting concentration.

3.4. Biofouling assessments

Biofilms formed on the membrane surface, cause decrease in permeance. In the first biofouling assessment, the apparatus and set up were sterilized initially, yet the rest of the experiment was carried out in a non-sterile environment. The pure water permeances of the membranes were determined and then the three PES membranes, three PES/PES-NHAc membranes, and three PES/PES-NClAc membranes were placed in seperate tanks filled with 0.1 CFU/mL *E. coli* BL21 solution. The flow was provided from the same stock with the same flow rate, 1 L/day. A set of membranes were left for biofouling for 1 day, and two sets of membranes were left for 2 days.

After one day one of each set was taken out, washed in distilled water, and the pure water permeances were measured. In the second day, the remaining two membranes were taken out, washed with distilled water, and pure water permeances were measured.

It was considered that the difference between the initial and final pure water permeances are because of the biofilm on the membranes. However, the results of PES showed another trend. Permeance of PES membranes after contact with bacterial solutions are much more than clean membranes. It could probably be because of the bacterial damage on the membrane. Since the skin layer is thinner than other membranes, and it has no antimicrobial activity, the chance that the PES

membrane was damaged by bacteria is higher. Then, the measured viscosity (0.6 dL/g) of the membrane's polymer showed no molecular weight change compared to pristine PES (see Appendix E). Then, it was suspected whether there was any change in hydrophilic/hydrophobic character of the biofouled membranes, and measured the contact angles of the membranes. We observed that there is no difference for PES membrane. On the other hand, PES/PES-NH_2 and PES/PES-NHAc membranes are slightly more hydrophobic than clean membranes (see Figure 50 in Appendix F).

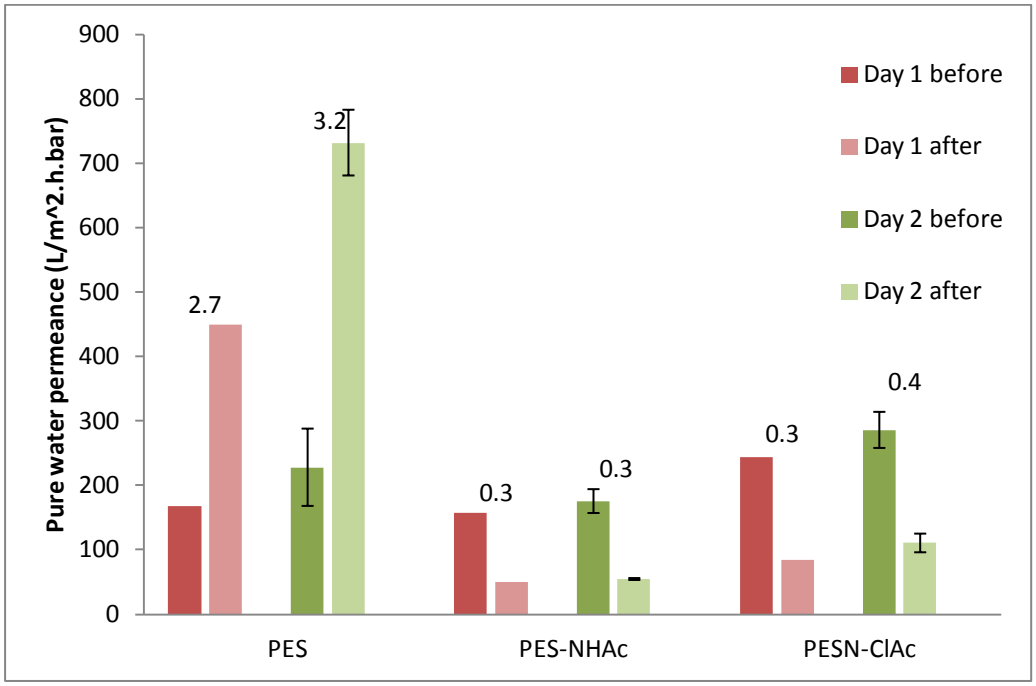

Figure 36. Pure water permeances before and after biofouling. PWP_{after}/PWP_{before} ratios are noted above the bars.

To compare the decrease, ratio of final to initial permeances were calculated and noted on the bars on the Figure 36. The ratios of PES/PES-NHAc and PES/PES-NClAc membranes indicate that chlorine was not efficient to prevent biofouling occurance, possibly due to the release of all chlorine in the first few hours.

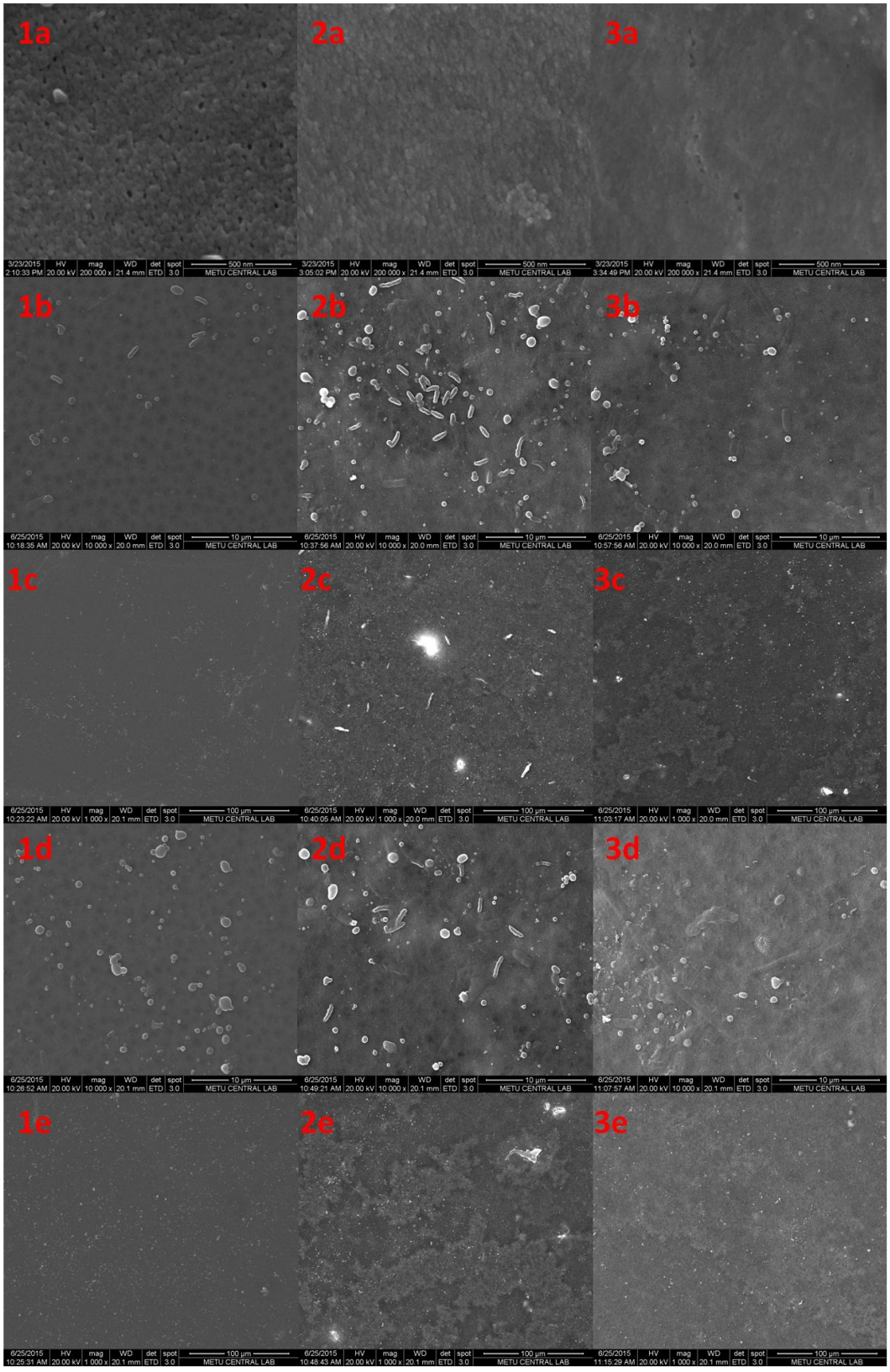

Figure 37. SEM images of of *E. coli* BL21 on 1) PES, 2) PES/PES-NHAc, and 3) PES/PES-NClAc membranes of a) clean membrane x200000 magnification, b) 24 h exposure x10000 magnification, c) 24 h exposure x1000 magnification, d) 56 h exposure x10000 magnification, and e) 56 h exposure x1000 magnification.

The second assessment was done under the same conditions with the first one. Apparatus and set up were sterilized initially, yet the rest of the experiment was carried out in a non-sterile environment. The biofilm analysis was done with SEM imaging (Figure 37). However, contamination by unknown microorganism(s) occured during the assessment, and two different cell structures were seen in SEM analysis. It was observed that all types of membranes were carrying bacteria, however biofilm formation was not observed in a wide range of area.

It is deduced that not only non-chlorinated membranes but also PES/PES-NClAc membranes were affected by bacteria. This is possibly because the bacteria to consumed all chlorine in few hours based on the chlorine release assessment. Yet, there are more bacteria settled and formed biofilm layer on PES/PES-NHAc membrane than PES/PES-NClAc membrane. The experiment was then repeated in sterile conditions.

In the third assessment, PES, PES/PES-NHAc, and PES/PES-NClAc membrane coupons were put in separate sterile vessels filled with *E. coli* stock solution. Then they were left to incubate for 48 h at 37^{o}C.

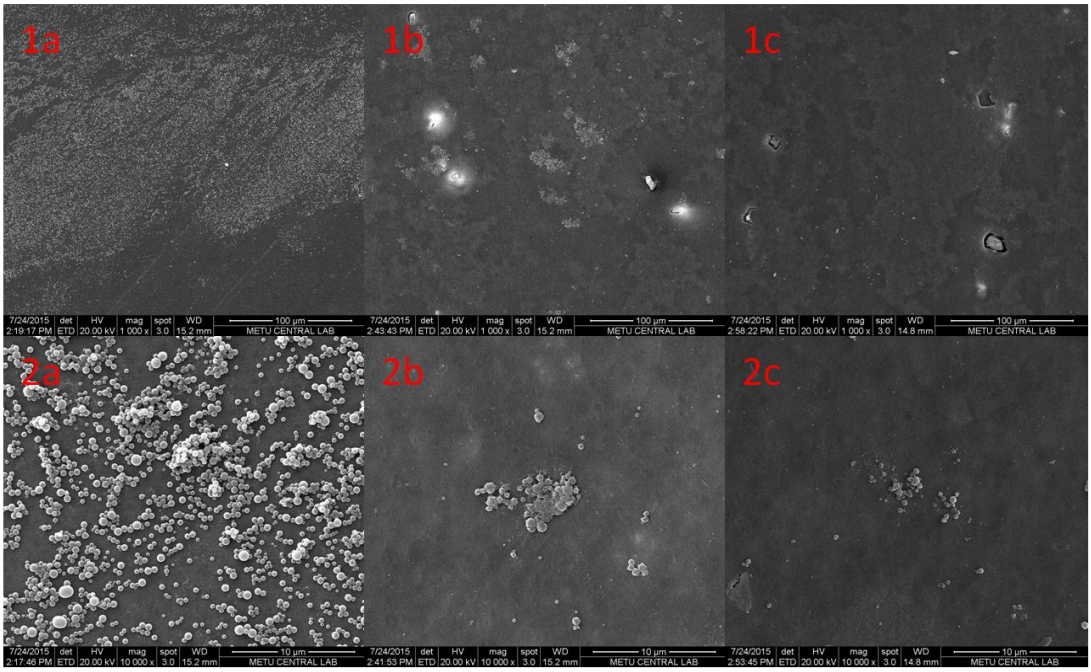

Figure 38. SEM images of *E. coli* BL21 on a) PES, b) PES/PES-NHAc, and c) PES/PES-NClAc membranes. 1) 1000x magnification, 2) 10 000x magnification.

The membranes were washed with 0.1 M PBS solution to remove loosely held bacteria, then placed in 3% gluteraldehyde solution for 24 hours to fix the cells on

the membranes. The membranes were dehydrated with ethanol and dried in vacuum oven. The surfaces were imaged by SEM. Selected images are shown in Figure 38.

It was observed that numerous bacteria were attached in a wide area on PES membrane. Although the PES/PES-NHAc membrane is not biocidally active, less bacteria attached to its surface than PES. This result could not be explained by biocidal effect and may be due to the hydrophilicity of the membrane.

The PES/PES-NClAc membrane showed less bacteria attached than PES/PES-NHAc. The biocidal activity of PES/PES-NClAc membrane may have affected the initial concentration of the bacteria, therefore interrupting the attachment and growth. Yet, they could not be inhibited totally.

CHAPTER 4:

CONCLUSIONS

4.1. Conclusions on chemical modifications

- Nitration, reduction, and acetylation reactions were successfully accomplished, and were confirmed by ATR FTIR and NMR spectrometers.
- The viscosity measurements of the polymers showed that the nitration reaction lowered the molecular weight of the polymer.
- Degree of nitration was calculated from the peak areas of NMR spectrum, as two nitro groups per repeating unit.
- 66% of nitro groups could be reduced to amino groups after the reduction reaction. This was calculated from the peak areas of NMR spectra.

4.2. Conclusions on membrane fabrication

- Since the modified polymers could not form membrane structure by themselves, PES/modified PES blends were prepared with the ratio of 10/6% respectively.
- After the modification, the membrane hydrophilicity was improved. The membrane permeance increased after the modification and blending process.
- Chlorination reactions were done on membranes using the modified polymers. Degree of chlorination was dependent on the concentration of HOCl solution. However, high concentration of HOCl damaged the membrane, and lowered its mechanical strength.
- Chlorination percentages were calculated as about 7% for PES/PES-NH_2 membrane, and about 12% for PES/PES-NHAc membrane.

4.3. Conclusions on biocidal and biofouling analysis

- Biocidal and biofouling analyses were done with membranes chlorinated from HOCl solutions with 5% active chlorine.
- The PES/PES-NCl_2 and PES/PES-NClAc membranes exhibited high antimicrobial property against *E.coli* BL21 and *Bacillus subtilis* in static antimicrobial tests.
- Antibiofouling property was examined on PES/PES-NClAc membrane. However, biofilm formation could not be achieved properly and repeatedly. Bacterial attachment on the membranes could be observed by SEM imaging, but an efficient antibiofouling property could not be observed.
- Chlorine release performance was improved by increasing chlorine loading on the membrane.
- If chlorine release time, chlorine concentration, and mechanical strength of modified PES membranes can be improved simultaneously, the antibiofouling properties can be improved as well.

REFERENCES

[1] Baker, R.W., Membrane Technology and Applications, 3rd edition, *John Wiley & Son*, **2012**, UK.

[2] Mulder, M., Basic Principle of Membrane Technology, 2nd Edition, Kluwer Academic Publishers, **1997**, Netherlands.

[3] Strathmann, H., Introduction to Membrane Science and Technology, Wiley-VCH, **2011**, Stuttgart.

[4] Edited by Osada Y., Nakagawa T., Membrane Science and Technology, *Marcel Dekker*, **1992**, New York.

[5] Botvay, A., Máthé, A., Pöppl, L., Nitration of Polyethersulfone by Ammonium Nitrate and Trifluoroacetic Anhydride, *Polymer*, **1999**, 40, 4965–4970.

[6] van der Bruggen, B., Chemical Modification of Polyethersulfone Nanofiltration Membranes: A Review, *Journal of Applied Polymer Science*, **2009**, 114, 630–642.

[7] Wang, D., Zhang, X., Nie, S., Zhao, W., Lu, Y., Sun, S., Zhao, C., Photoresponsive Surface Molecularly Imprinted Poly(ether sulfone) Microfibers, *Langmuir*, **2012**, 28, 13284−13293.

[8] Çulfaz, P.Z., Microstructured Hollow Fibers and Microsieves Fabrication, Characterization and Filtration Applications, PhD Dissertation, University of Twente, **2010**, Netherlands.

[9] Lewandowski, Z., Beyenal, H., Fundamentals of Biofilm Research, CRC Press, **2007**, USA.

[10] Yu, Q., Wu, Z., Chen, H., Dual-function Antibacterial Surfaces for Biomedical Applications, *Acta Biomaterialia*, **2015**, 16, 1-13.

[11] Chapman, R.G., Ostuni, E., Liang, M.N., Meluleni, G., Kim, E., Yan, L., Pier, G., Warren, H.S., Whitesides, G.M., Polymeric Thin Films That Resist the Adsorption of Proteins and the Adhesion of Bacteria, *Langmuir*, **2001**, 17, 1225-1233.

[12] Cheng, G., Zhang, Z., Chen, S., Bryers, J.D., Jiang, S., Inhibition of bacterial adhesion and biofilm formation on zwitterionic surfaces, *Biomaterials*, **2007**, 28, 4192–4199.

[13] Kuroki, H., Tokarev, I., Minko, S., Responsive Surfaces for Life Science Applications, *Annu. Rev. Mater. Res.*, **2012**, 42, 343-372.

[14] Lemire1, J.A., Harrison, J.J., Turner, R.J., Antimicrobial Activity of Metals: Mechanisms, Molecular Targets and Applications, *Nature Reviews*, **2013**, 11, 371-384.

[15] Yin, J.,Yang, Y., Hua, Z., Deng, B., Attachment of Silver Nanoparticles (AgNPs) onto Thin-Film Composite (TFC) Membranes Through Covalent Bonding to Reduce Membrane Biofouling, *Journal of Membrane Science*, **2013**, 441, 73-82.

[16] Kamışoğlu, K., Aksoy, E.A., Akata, B., Hasırcı, N., Baç, N., Preparation and Characterization of Antibacterial Zeolite–Polyurethane Composites, *Journal of Applied Polymer Science*, **2008**, 110, 2854–2861.

[17] Zhang, T., Zhu, C., Maa, H., Li, R., Dong, B., Liu, Y., Li, S., Surface Modification of APA-TFC Membrane with Quaternary Ammonium Cation and Salicylaldehyde to Improve Performance, *Journal of Membrane Science*, **2014**, 457, 88-94.

[18] Li, C., Liu, Y., Zeng, Q-Y., Ao, N-J., Preparation and Antimicrobial Activity of Quaternary Phosphonium Modified Epoxidized Natural Rubber, *Materials Letters*, 2013, 93, 145–148.

[19] Kovacic, P., Lange, R.M., Foote, J.L., Goralski, C.T., Hiller, Jr., J.J.H., Levinsky, J.A., A New Method of Aromatic Substitution Yielding Unusual

Orientation. Amination with N-Haloamines Catalyzed by Aluminum Chloride, *Communications to The Editor*, **1963**, 86, 1650-1651.

[20] Kovacic, P., Lowery, M.K., Field, K.W., Chemistry of N-Bromoamines and N-Chloroamines, *Chemical Reviews*, **1970**, Vol 70, 6, 639-665.

[21] Hui, F., Debiemme-Chouvy, C., Antimicrobial N‑Halamine Polymers and Coatings: A Review of Their Synthesis, Characterization, and Applications, *Biomacromolecules*, **2013**, 14, 585-601.

[22] Gutman, O., Natan, M., Banin, E., Margel, S., Characterization and antibacterial properties of N-halaminederivatized cross-linked polymethacrylamide nanoparticles, *Biomaterials*, **2014**, 35, 5079-5087.

[23] Ahmed, A.E.I., Cavalli, G., Bushell, M.E., Wardell, J.N., Pedley, S., Charles, K., Hay, J.N., New Approach To Produce Water Free of Bacteria, Viruses, and Halogens in a Recyclable System, *Appl. Environ. Microbiol.,* **2011**, Vol 77, 3, 847-853.

[24] Sun, G., Allen, L.C., Luckie, E.P., Wheatley, W.B., Worley, S.D., Disinfection of Water by N-Halamine Biocidal Polymers, *Ind. Eng. Chem. Res.*, **1995**, 34, 4106-4109.

[25] Xu, J., Wanga, Z., Yu, L., Wanga, J., Wanga, S., A Novel Reverse Osmosis Membrane with Regenerable Anti-biofouling and Chlorine Resistant Properties, *Journal of Membrane Science*, **2013**, 435, 80–91.

[26] Ren, X., Akdag, A., Kocer, H.B., Worley, S.D., Broughton, R.M., Huang, T.S., N-Halamine-Coated Cotton for Antimicrobial and Detoxification Applications, *Carbohydrate Polymers*, **2009**, 78, 220–226.

[27] Cao, Z., Sun, Y., Polymeric *N*-Halamine Latex Emulsions for Use in Antimicrobial Paints, *Applied Materials and Interfaces*, **2009**,Vol. 1, No. 2, 494–504.

[28] Hendrick, C.E., Wang, Q., Synthesis of ortho-Haloaminoarenes by Aryne Insertion of Nitrogen-Halide Bonds, *J. Org. Chem.*, **2015**, 80, 1059−1069.

[29] Kim, C., Cha, Y-N., Taurine Chloramine Produced From Taurine Under Inflammation Provides Anti-inflammatory and Cytoprotective Effects, *Amino Acids*, **2014**, 46, 89-100.

[30] Marcinkiewicz, J., Kontny, E., Taurine and Inflammatory Diseases, *Amino Acids*, **2014**, 46, 7-20.

[31] Schuller-Levis, G.B., Park, E., Taurine: New Implications for an Old Amino Acid, *FEMS Microbiology Letters*, 2003, 226, 195-202.

[32] Wang, D., Zhang, X., Nie, S., Zhao, W., Lu, Y., Sun, S., Zhao, C., Photoresponsive Surface Molecularly Imprinted Poly(ether sulfone) Microfibers, *Langmuir*, **2012**, 28, 13284-13293.

[33] Akdağ, A., Okur, Ş., McKee, M.L., Worley, S.D., The Stabilities of N-Cl Bonds in Biocidal Materials, *J. Chem. Theory Comput.*, **2006**, 2, 879-884.

[34] Ahmed, A.E.I., Hay, J.N., Bushell, M.E., Wardell, J.N., Cavalli, G., Optimizing Halogenation Conditions of N-Halamine Polymers and Investigating Mode of Bactericidal Action, *Journal ofApplied Polymer Science*, **2009**, 113, 2404–2412.

[35] Akdağ, A., Koçer, H.B., Worley, S.D., Broughton, R.M., Webb, T.R., Bray, T.H., Why Does Kevlar Decompose, while Nomex Does Not, When Treated with Aqueous Chlorine Solutions?, *J. Phys. Chem.*, **2007**, 111, 5581-5586.

[36] Yu, H., Zhang, X., Zhang, Y., Liu, Jindun, Zhang, H., Development of a hydrophilic PES ultrafiltration membrane containing SiO_2@*N*-halamine nanoparticles with both organic antifouling and antibacterial properties, *Desalination*, **2013**, 326, 69-76.

[37] Philippides, A., Budd, P.M., Price, C., Cunclifte, V., The nitration of polystyrene, *Polymer*, **1993**, 34, 16, 3506-3513.

[38] Nazri, N.A.M., Lau, W.J., Ismail, A.F., Improving water permeability and anti-fouling property of polyacrylonitrile-based hollow fiber ultrafiltration membranes by surface modification with polyacrylonitrile-*g*-poly(vinyl alcohol) graft copolymer, *Korean J. Chem. Eng*., **2015**, 32, 9, 1853-1863.

[39] Li, F., Yea, J., Yanga, L., Denga, C., Tiana, Q., Yang, B., Surface modification of ultrafiltration membranes by grafting glycine-functionalized PVA based on polydopamine coatings, *Applied Surface Science*, **2015**, 345, 301–309.

[40] Miller, D.J., Araújo, P.A., Correia, P.B., Ramsey, M.M., Kruithof, J.C., van Loosdrecht, M.C.M., Freeman, B.D., Paul, D.R., Whiteley, M., Vrouwenvelder, J.S., Short-term adhesion and long-term biofouling testing of polydopamine and poly(ethylene glycol) surface modifications of membranes and feed spacers for biofouling control, *Water Research*, **2012**, 46, 3737-3753.

APPENDIX A:

FTIR SPECTRA

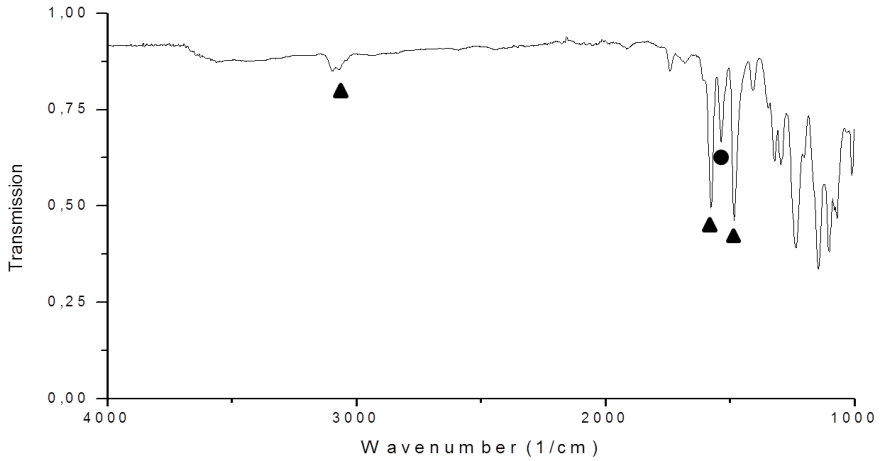

Figure 39. FTIR spectrum of PES-NO_2 (b). (1536 cm^{-1})

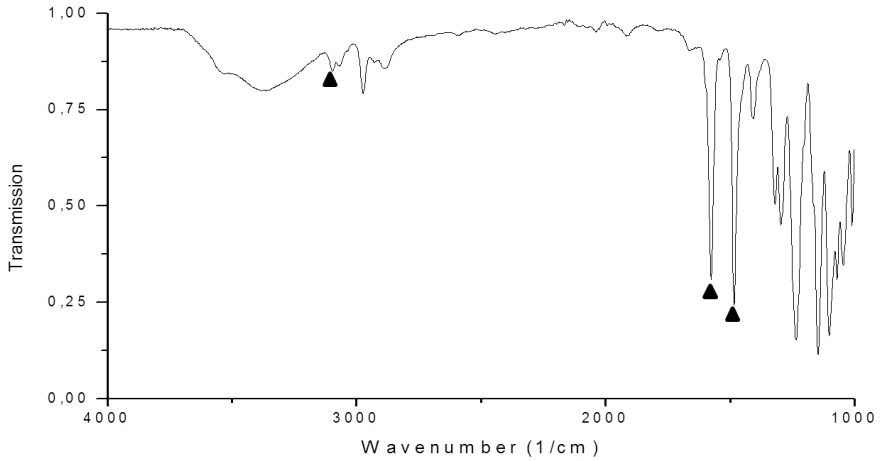

Figure 40. FTIR spectrum of PES-NO_2 (c).

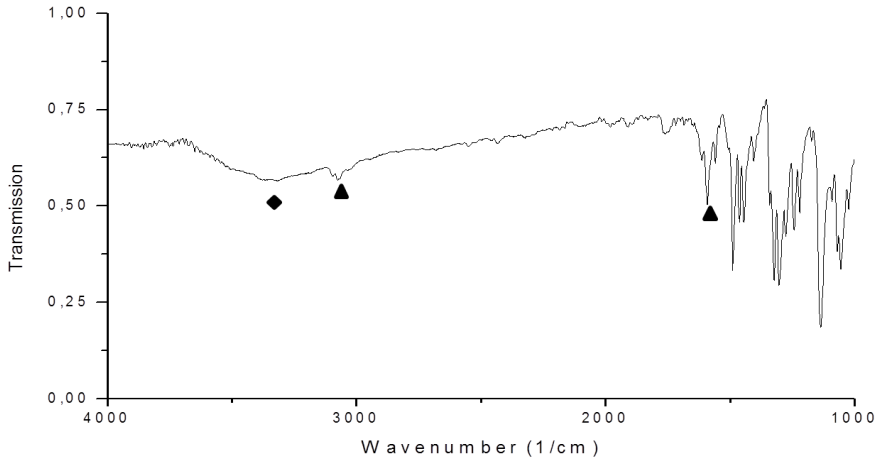

Figure 41. FTIR spectrum of PES-NH_2 (b). (3350 cm^{-1})

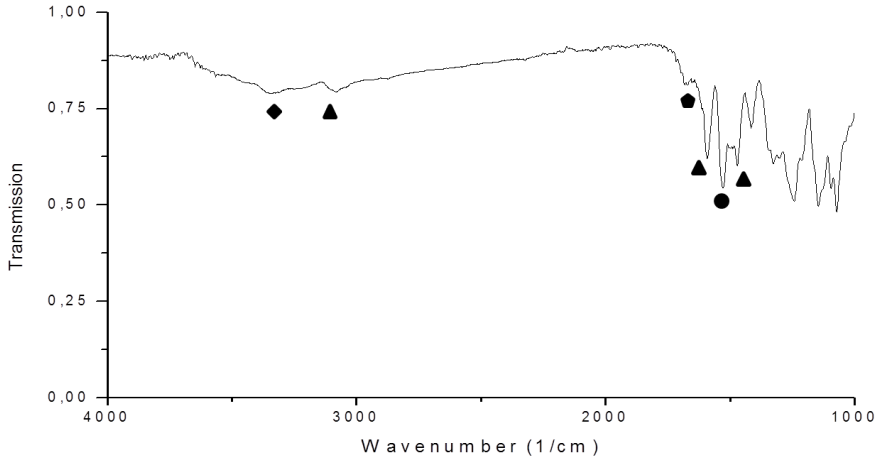

Figure 42. FTIR spectrum of PES-NHAc (b). (1673 cm^{-1})

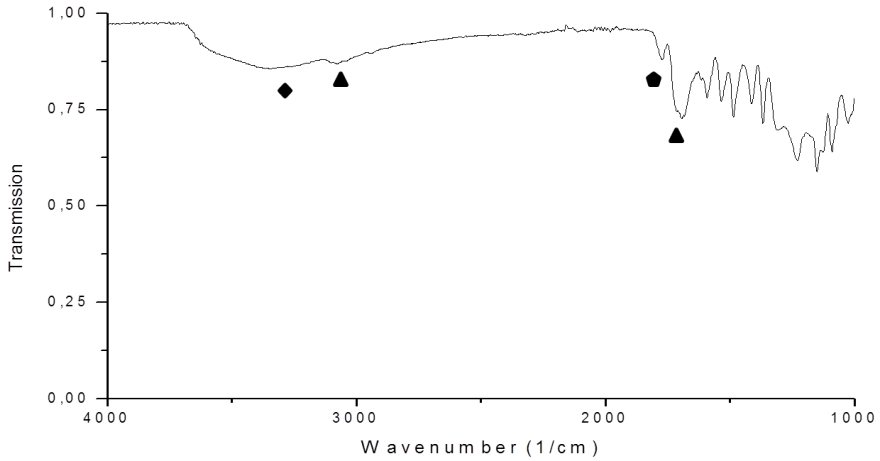

Figure 43. FTIR spectrum of PES-NHAc (c). (1682 cm^{-1})

In FTIR figures, ▲ represents the characteristic peaks of PES. ● represents the new peak appeared after nitration reaction of PES. ◆ represents the new peak appeared after reduction reaction of PES-NO_2. ⬟ represents the new peak appeared after acetylation reaction of PES-NH_2.

The FTIR spectra of membranes are:

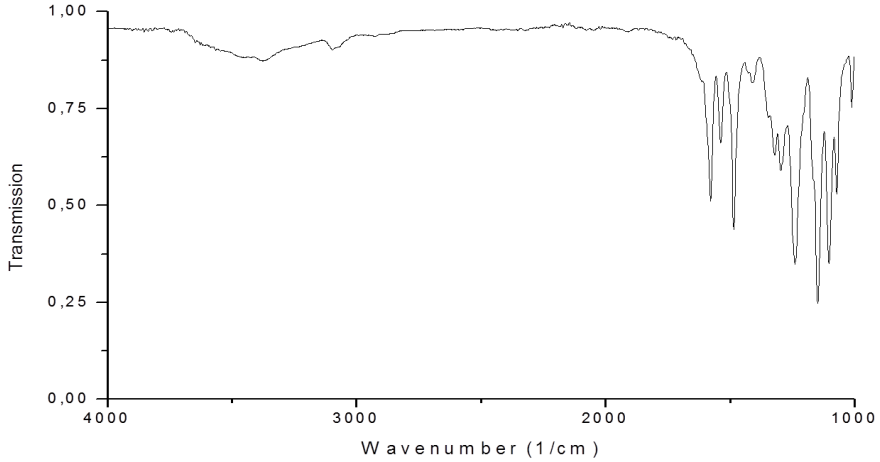

Figure 44. FTIR spectrum of PES/PES-NH_2 membrane.

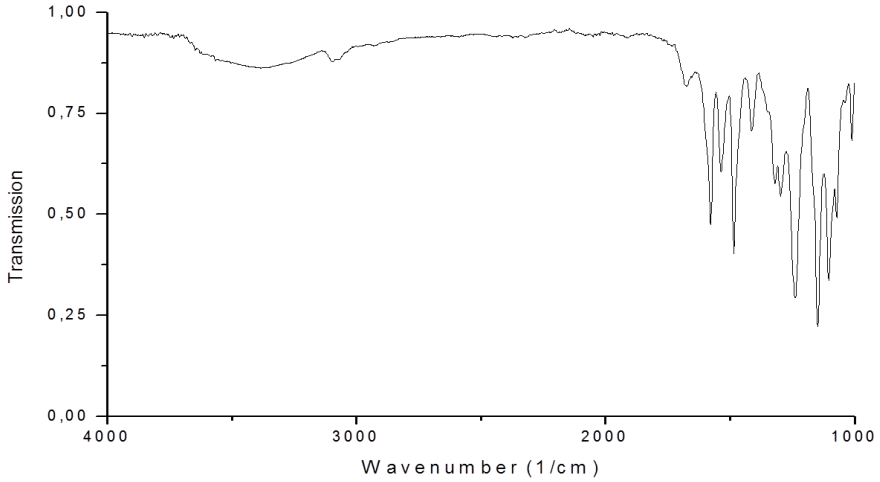

Figure 45. FTIR spectrum of PES/PES-NHAc membrane.

APPENDIX B:

CHLORINE ASSESSMENTS

PES/PES-NCl_2 and PES/PES-NClAc membranes were prepared by chlorination of PES/PES-NH_2 and PES/PES-NHAc membranes, respectively. Chlorine charge and recharge is an equilibrium process, which takes place as follows:

$$R_2N - H + HOCl \leftrightarrow R_2N - Cl + H_2O$$

Chlorine amount on a membrane was determined by iodometric titration method.

Iodometric titration is a chemical way to obtain oxidative species quantitativaly. In the case of this thesis, iodide is oxidized by chlorine to molecular iodine. Iodine is reduced back to iodide by the titrant, sodium thiosulfate ($Na_2S_2O_3$). During this reaction occurs, starch is added to the medium as an indicator. Starch makes a complex with molecular iodine giving blue color to the medium, however iodide is colorless. The presence of chlorine, iodide and starch in a medium results in blue color. The chlorine amount is calculated stoichiometrically from the volume of titrant added.

The reaction takes place as follows:

$$OCl^- + 3I^- + 2H^+ \xrightarrow{starch} Cl^- + I_3^- + H_2O$$

$$I_3^- + 2\,S_2O_3^{2-} \xrightarrow{starch} 3\,I^- + S_4O_6^{2-}$$

The chlorine amount is calculated as:

$$n_{Cl^+} = \frac{V_{NaS_2O_3} * M_{NaS_2O_3}}{2} * m_{Cl}$$

where n_{Cl^+} is mole of active chlorine, $V_{NaS_2O_3}$ is volume of the titrant NaS_2O_3, $M_{NaS_2O_3}$ is molarity of the titrant, m_{Cl} is atomic weight of the chlorine.

Chlorination percentage is calculated as:

$$Cl\% = \frac{n_{Cl}}{m_{membrane} x \frac{6\ g\ modified\ PES}{16\ g\ blend\ in\ membrane} x 66\%\ (NH_2\ group) x \frac{1}{Mw_{repeating\ unit}} x \frac{4n_H}{1n_{repeating\ unit}}} x100$$

where *Cl%* is chlorine percent calculated; $m_{membrane}$ is the weight of a membrane coupon; $Mw_{repeating\ unit}$ is the molecular weight of the repeating unit; $n_H/n_{repeating\ unit}$ the mole ratio of hydrogen atom bonded to nitrogen per repeating unit, that is equal to 4.

The dope solution that membrane was made up of 10 wt % PES, and 6 wt % PES-NH_2, therefore the weight of the membrane multiplied with 6/16 with the assumption of the membrane includes PES-NH_2 with 6/16 ratio. It was mentioned that the modified polymer ratio reduces during the membrane formation. Consequently, the chlorine contents of the membranes are minimum chlorination percentages.

The reduction ratio was calculated from ^{1}H NMR analysis as 0.66. To calculate PES-NH_2 repeating unit, it is multiplied by 0.66. Each succeffully reduced repeating unit has 4 *N*-halamine hydrogen per repeating unit. The mole ratio of them is equal to 4. In order to calculate the mole of repeating unit, the weight of the PES-NH_2 was divided to molecular weight of the repeating unit. In conclusion, mole of chlorine loaded was divided into mole of total *N*-halamine hydrogen, then multiplied by 100.

For the calculation of PES-NHAc, it was assumed that 50% acetylation occured, since the exact acetylation ratio was not known. It was assumed that a repeating unit includes an amine and an amide group. The hydrogen number that can undergo chlorination was taken as 3, and the molecular weight calculated based on this assumption. The rest of the calculation was made the same with the PES-NH_2 one.

The raw data of Figure 26 and Figure 27 are listed below.

Table 8. Chlorination assessment raw data.

	PES/PES-NH_2		
Active chlorine % / Time (min)	**10**	**60**	**120**
0.3	2.0	2.6	1.6
	1.8	1.8	1.8
1	5.8	4.5	3.7

	6.6	6.2	4.7
5	7.9	8.0	5.9
	9.8	7.0	4.5
10	11.0	8.6	7.2
	10.7	10.6	8.8
15	15.1	13.7	7.2
	11.6	16.4	8.2

	PES/PES-NHAc		
Active chlorine % / Time (min)	**10**	**60**	**120**
0.3	4.6	2.4	2.2
	2.7	1.9	1.8
1	7.6	5.7	5.8
	5.3	0	7.8
5	11.3	12.3	7.6
	9.4	10.5	9.0
10	13.8	13.7	9.5
	11.7	13.2	8.7
15	12.6	13.7	8.3
	13.3	13.3	9.3

Table 9. PES/PES-NCl_2 (5%) membrane chlorine release in water assessment raw data of Figure 28.

Time (min)	Cl (mg)/membrane (g)	Time (min)	Cl (mg)/membrane (g)
0	1.5	249	1.0
0	1.9		0.8
0	1.8		0.8
60	1.6	304	0.6
	1.8		0.8
	1.2		0.3
107	1.5	360	0.1
	1.8		0.4
	1.3		0.3
198	0.9	439	0.0
	0.9		0.2
	0.4		0.0

Table 10. PES/PES-NClAc (5%) membrane chlorine release in water assessment raw data of Figure 28.

Time (min)	Cl (mg)/ Memb. (g)	Time (min)	Cl (mg)/ Memb. (g)	Time (min)	Cl (mg)/ Memb. (g)
0	5.1	346	3.2	919	1.3
0	6.7	346	3.1	919	1.7
0	4.8	346	2.7	919	1.8
94	3.0	543	3.1	1003	1.9
94	3.1	543	2.6	1003	2.0
94	2.4	543	3.0	1003	2.0
188	2.7	636	1.9	1097	1.9
188	2.1	636	2.1	1097	1.1
188	2.2	636	1.7	1097	1.1
263	2.6	745	1.8	1315	1.7
263	3.2	745	2.1	1315	1.2
263	3.1	745	2.3	1315	1.5

Table 11. PES/PES-NClAc (5%) membrane chlorine release in 10^5 CFU/mL *E.coli* solution assessment raw data of Figure 29.

Time (min)	Chlorine (mg)/ membrane(g)	Time (min)	Chlorine (mg)/ membrane(g)
0	15.6	177	1.3
0	16.3	177	1.9
0	17.0	177	1.4
0	17.3	250	0.0
63	4.9	250	0.2
63	3.8	250	0.0
63	3.4	333	0.0
124	1.5	333	0.0
124	4.0	333	0.0
124	6.3		

Table 12. PES/PES-NClAc (5%) membrane chlorine release in 10^8 CFU/mL *E.coli* solution assessment raw data of Figure 29.

Time	Chlorine (mg)/membran (g)
0	5.2
0	5.4
0	5.7
0	6.6
0	5.8
94	2.5
94	0.0
94	1.4
118	0.0
118	0.1
118	0.0
175	0.0
175	0.0
175	0.0

Table 13. PES/PES-NClAc (15%) membrane chlorine release in 10^8 CFU/mL *E.coli* solution assessment raw data of Figure 29.

Time (min)	Chlorine (mg) / membrane (g)	Time (min)	Chlorine (mg) / membrane (g)
0	15.1	172	3.9
0	17.2	172	7.5
0	13.0	172	3.0
38	9.8	214	2.5
38	7.8	214	6.2
38	9.2	214	2.9
71	4.4	262	0.7
71	5.5	262	3.3
71	4.2	262	2.4
108	11.7		
108	8.4		
108	6.9		

APPENDIX C:

GROWTH CURVE ANALYSIS

For biocidal analysis of materials, the growth curve of the bacteria is derived. Bacteria show a growth behaviour in time after inoculation in a nutrient medium. A typical growth curve is shown in Figure 46. The growth curve consists of six phases. In the lag phase, bacteria adaptates it metabolism to the environment. In the starting phase, the adaptation occurs and the cells start to reproduce. In the exponential phase, the number of cells increases exponentially. In the slow-down or decelerate phase, the growth of the cells slows-down. It is because the essential nutrients start to deplete, or cells accumulate toxic products to the environment. In the stationary phase, the growth and death of the bacteria are in balance. In the die-off phase, the bacterial concentration reduces [10].

For an antimicrobial assessment of a material, the growth phase of the bacteria should be in the range of exponential and stationary phases. Since the cells in the lag and starting phases are too sensitive, and in the die-off phase are already tend to die. In order the experiment to be reliable, the cells are suppose to be healthy.

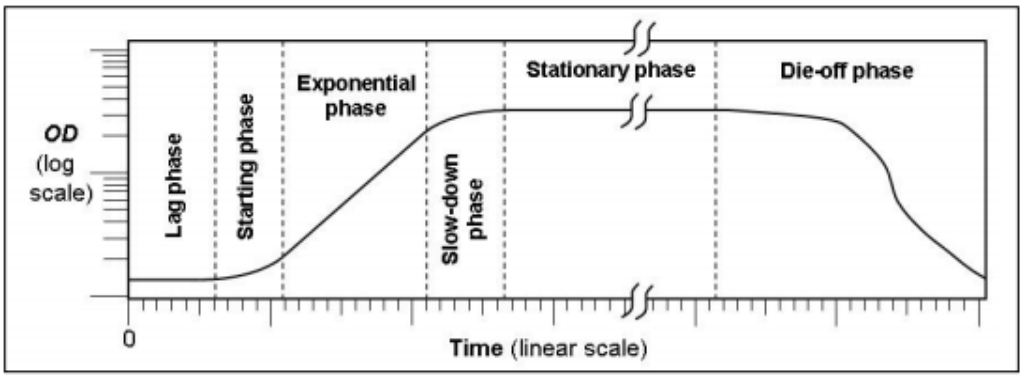

Figure 46. A typical growth curve.

For biocidal assessments, we should apply biocidal material due exponential phase. Since, we have to be sure that cells die not naturally, but intentionally.

The absorbance was measured once an hour, and growth curve was generated as:

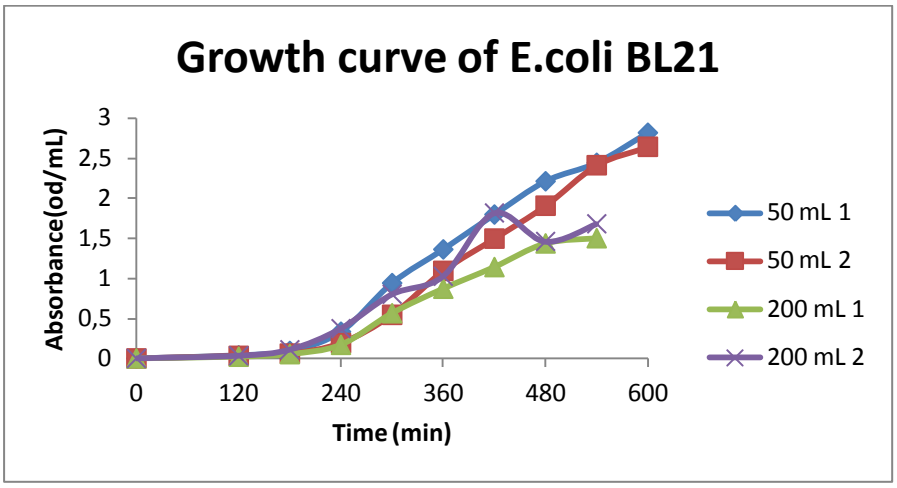

Figure 47. Growth curve of *E.coli* BL21 in different volume of LB Broth solutions (20 g/mL).

We took start of exponential phase at around 5th hour.

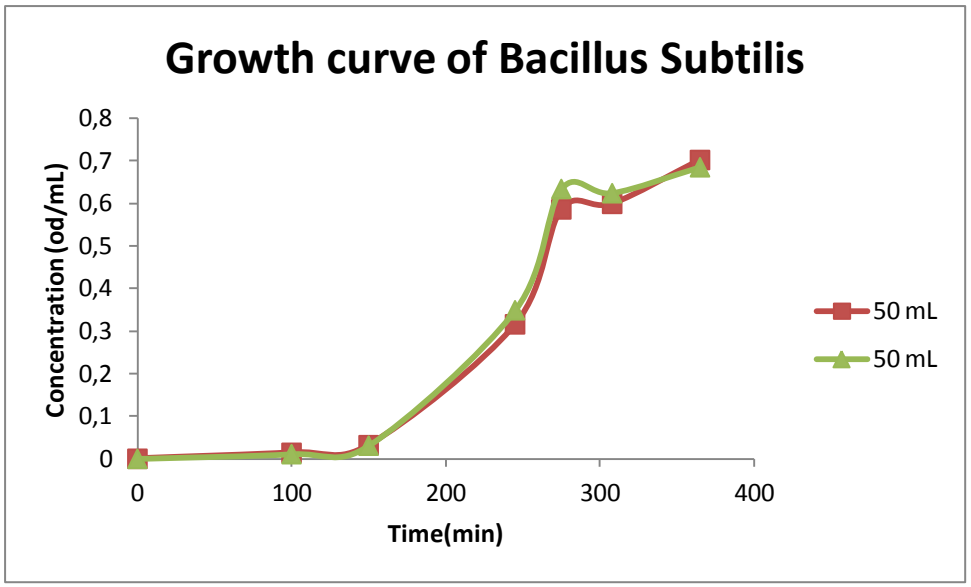

Figure 48. Growth curve of *Bacillus* subtilis in two sets of 50 mL of LB Broth solutions (20 g/mL).

We took exponential phase initiates at around 3.5th hour.

APPENDIX D:

OTHER BIOFOULING ASSESSMENTS

D.1. Total Organic Carbon measurement

0.92 g sodium acetate, 0.10 g sodium dihydrogen phosphate, 0.33 g sodium nitrate was dissolved in tap water as a feed solution [40]. Tap water was chosen as a natural bacteria source. The solution was distributed to 5 different tubes. Then four coupons for each of PES, PES/PES-NH_2, PES/PES-NHAc, PES/PES-NCl_2, and PES/PES-NClAc membrane coupons were placed into the solutions. Once a week one of the coupons were taken, washed with ultra pure water. Afterwards, vortexed for a minute and ultrasonicated for three minutes, which cycled three times. Any deposition on the membrane surface were transferred to water in this way. Then, Total Organic Carbon (TOC) measurements were done.

It was expected the feed solution was contaminated from the water and the environment. Therefore, the membranes were going to biofoul in nutrient medium described. Then the bacteria attached to the surface were transferred to ultrapure water by vortexing and ultrasonication.

Total carbon and inorganic carbon amounts were measured by the instrument and the difference was taken as organic carbon. The organic carbon amount was taken as proportional with the amount of the bacteria.

It was expected that chlorinated membranes show less TOC than non-chlorinated membranes in initial weeks, but increases in the progressing weeks. However, there was no regular behaviour in the results, which are shown in Figure 49. That may be because the polymers are also organic compounds, during the vortex and ultrasonication, polymers may leave the membrane structure and involved in the solution analyzed. However, the polymer concentration in analyt may not be standart.

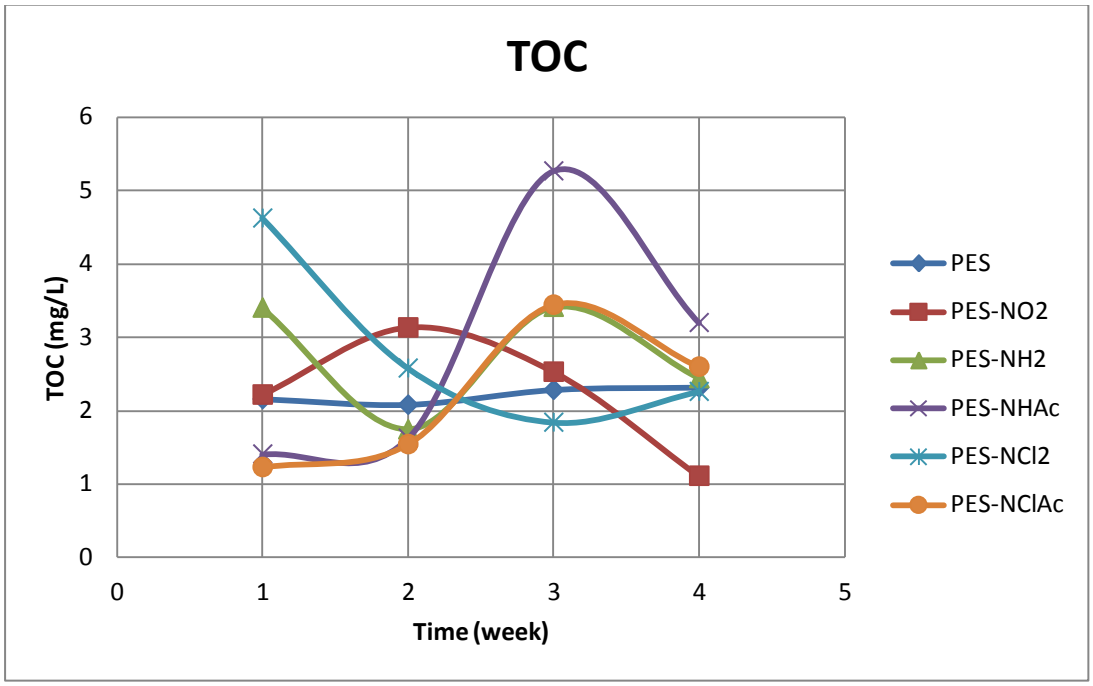

Figure 49. Total Organic Carbon amounts of the biofouled membranes in four weeks.

D.2. Increase in resistance

Fouling and biofouling increase the energy needed, or decreases the permeance flux of the purification process. In this experiment, initially an LB Broth liquid nutrient solution concentration and flux velocity was optimized as not causing to fouling, which was decided as 5 g/L LB Broth at 1 L/h flux. Then *E. coli* BL21 was incubated in the feed solution to 0.1 CFU/mL.

Fouling behaviour of PES, PES/PES-NHAc, PES/PES-NClAc membranes were examined with that infected solution. Instant flux and trans membrane pressure (TMP) were recorded and resistances were calculated by using Darcy's law:

$$R = \frac{\Delta P}{\eta . J}$$

where R is resistance, ΔP is pressure gradient, η is viscosity,and J is permeance.

Total resistance is sum of membrane resitance, R_{mem}, and fouling resistance, R_{foul}.

$$R_{total} = R_{mem} + R_{foul}$$

Membrane resistances were initially determined with pure water permeation, then fouling experiments was carried out, and fouling resistances were calculated. Increasing of the resistance in time is shown in Figure 50.

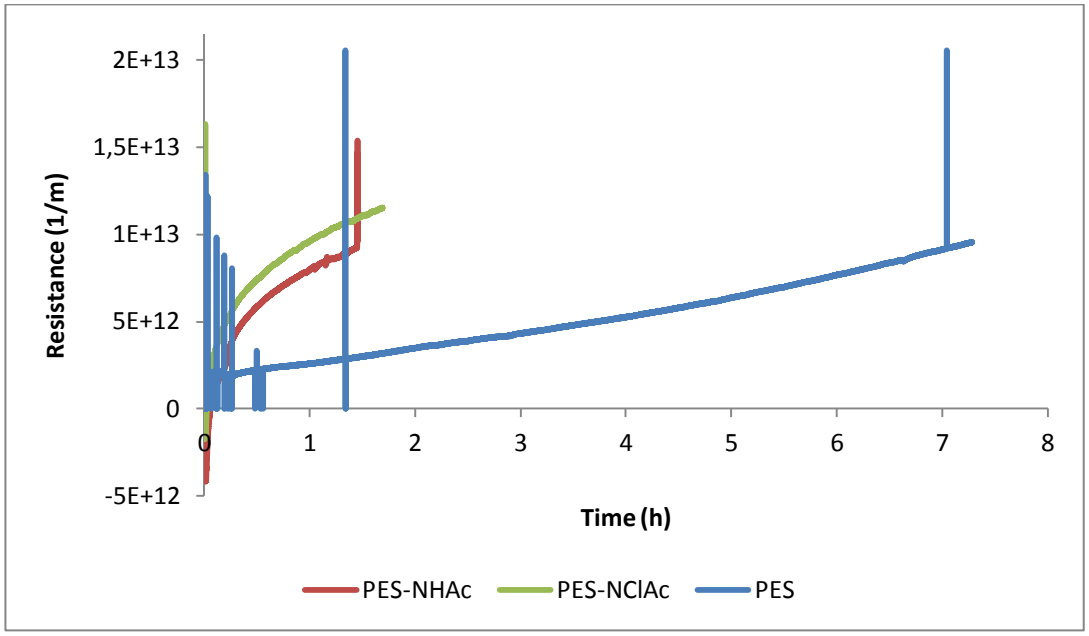

Figure 50. Fouling resistances of PES, PES/PES-NHAc, and PES/PES-NClAc membranes in time.

It was observed that resistance of PES membrane increases in a regular manner, and less than modified PES membranes. Whereas, resistances of PES/PES-NHAc and PES/PES-NClAc membranes increases rapidly. Since the pressure gradient at most can be 1, the experiment could not be pursued more. The time span of the experiment was not efficient to form biofilm on the membranes, that indicates the resistance gradients were only because of fouling of the bacteria.

Therefore we concluded that this experiment set up was inefficient to analyse biofilm occurance on the membranes.

APPENDIX E:

VISCOSITY MEASUREMENTS

Molecular weights of high molecular weight polymers are determined with several ways. One of them is Ubbelohde capillary viscometer. The ratio of flow times of solvent and polymer solution gives the relative viscosity (η_{rel}). When the natural logarithm of relative viscosities of polymer solutions at different concentrations are plotted, the intercept gives the intrinsic viscosity ($[\eta]$) of the polymer. Kreamer equation is as follows:

$$\frac{ln\eta_{rel}}{C} = [\eta] + k_H[\eta]^2 C$$

Viscosity average molecular weights of the polymers are calculated with intrinsic viscosity values depending on Mark-Houwink-Sakurada equation:

$$[\eta] = KM^{\alpha}$$

In order to examine the difference in molecular weight, we measured the viscosities of PES, PES-NO_2, PES-NH_2, and PES-NHAc in DMF. First, the flow time of DMF was determined for a particular volume. Afterwards, flow times of 0.5 g/dL polymer solutions were determined for the same particular volume. The flow times of 0.4 g/dL, and 0.3 g/dL solutions were determined as well. Then, the relative viscosities of each measurement were calculated by dividing the flow time of polymer to flow time of solvent (t_{poly} / t_{DMF}).

From Figure 49 the intrinsic viscosities are calculated as $[\eta]_{\mathrm{PES}} = 0.6$ dL/g, $[\eta]_{\mathrm{PES-NO_2}} = 0.16$ dL/g, $[\eta]_{\mathrm{PES-NH_2}} = 0.21$ dL/g, $[\eta]_{\mathrm{PES-NHAc}} = 0.19$ dL/g.

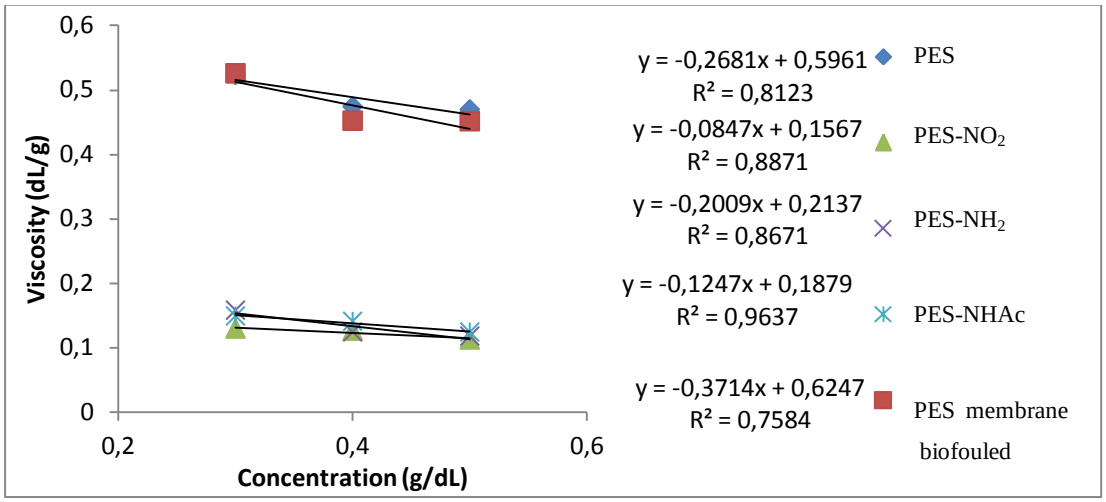

Figure 51. Intrinsic viscosity calculation of the polymers.

APPENDIX F:

OTHER EXPERIMENTAL DATA

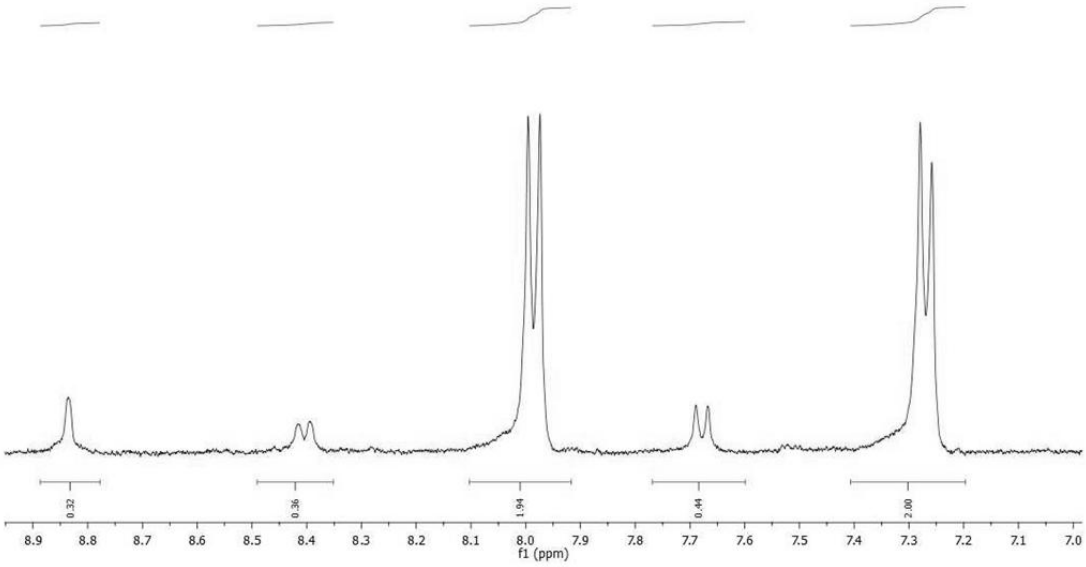

Figure 52. ^{1}H NMR spectrum of PES/PES-NH_2 membrane.

$$\frac{PES - NH_2}{PES} = \frac{Total\ peak\ area\ of\ modified\ PES/3}{Total\ peak\ area\ of\ PES/4} = \frac{1.12/3}{3.94/4} = \frac{4}{10}$$

Total peak areas of modified PES is equal to 1.12 (sum of 0.32, 0.36, and 0.44). These peaks are arising from three different protons, therefore the area is divided to three. The total peak areas of PES is equal to 3.94 (sum of 1.94 and 2.00). These peaks are arising from four different protons, therefore the area is divided to four.

The ratio of a proton area of modified PES to a proton area of PES is equal to 4/10. This is the ratio of PES-NH_2/PES in the membrane.

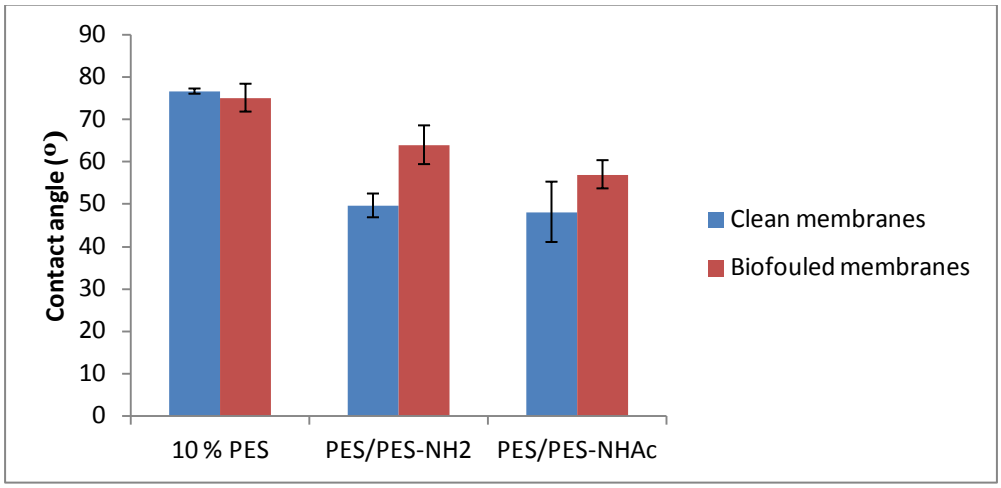

Figure 53. Contact angles of clean membranes and after bacterial exposure.

The thermal analysis of the polymers were done. T_g of PES was determined as 230 as expected. However the T_g of modified polymers could not be obtained clearly.

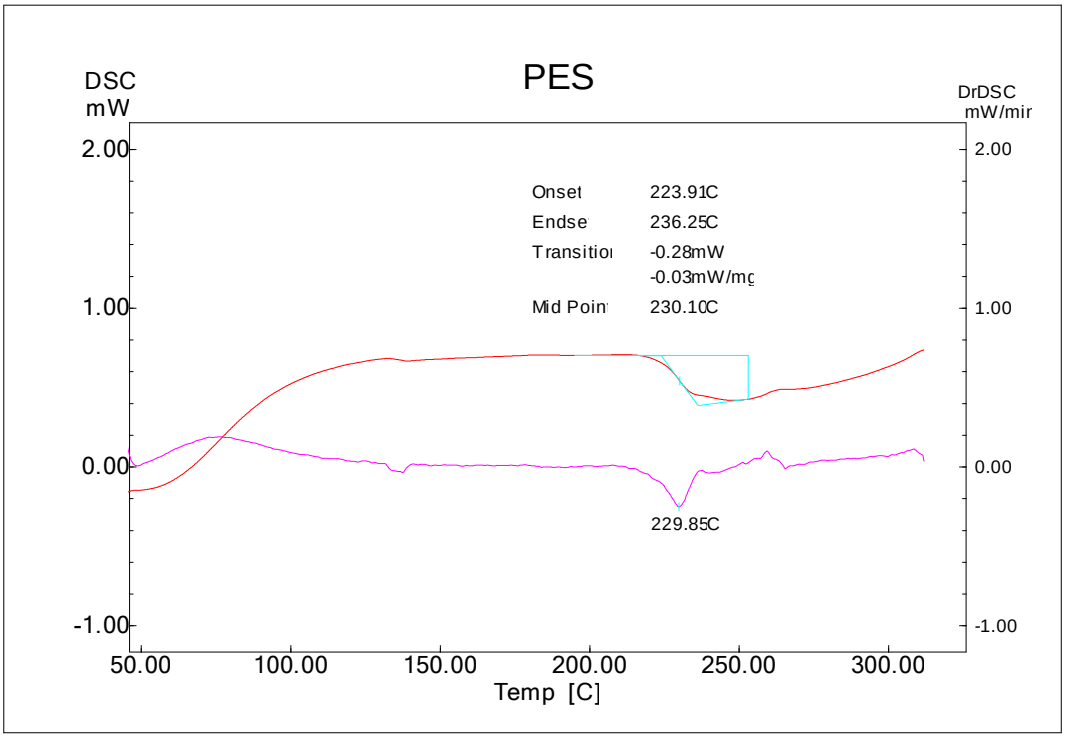

Figure 54. DSC graph of PES.

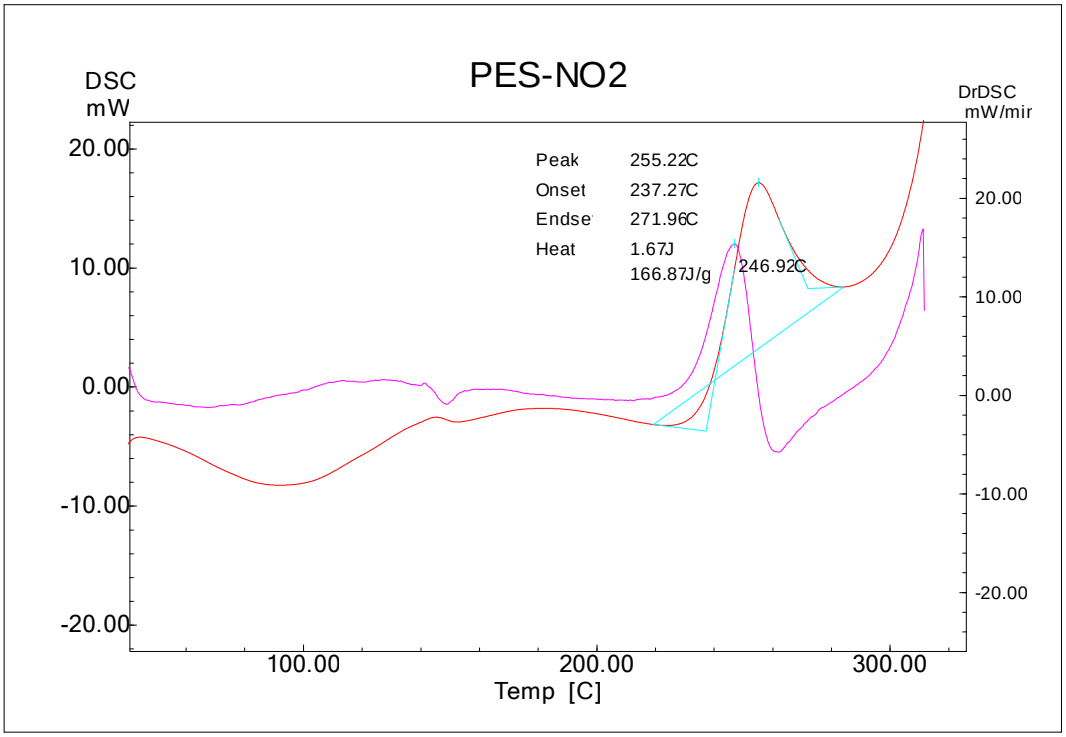

Figure 55. DSC graph of PES-NO_2.

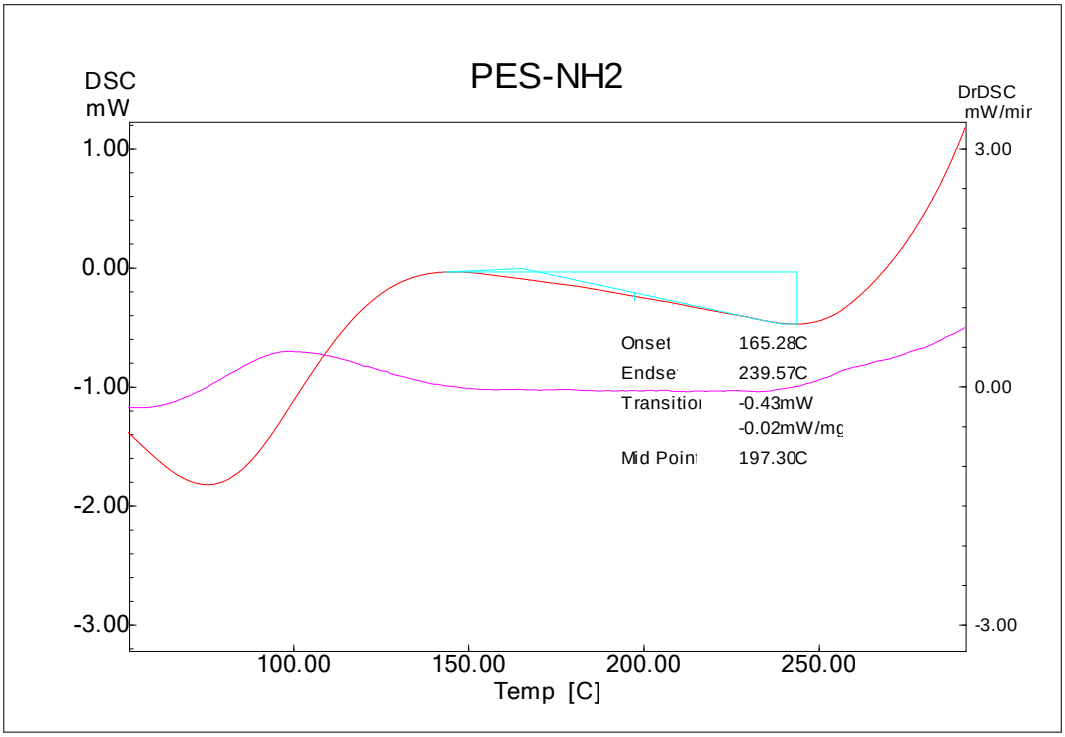

Figure 56. DSC graph of PES-NH_2.

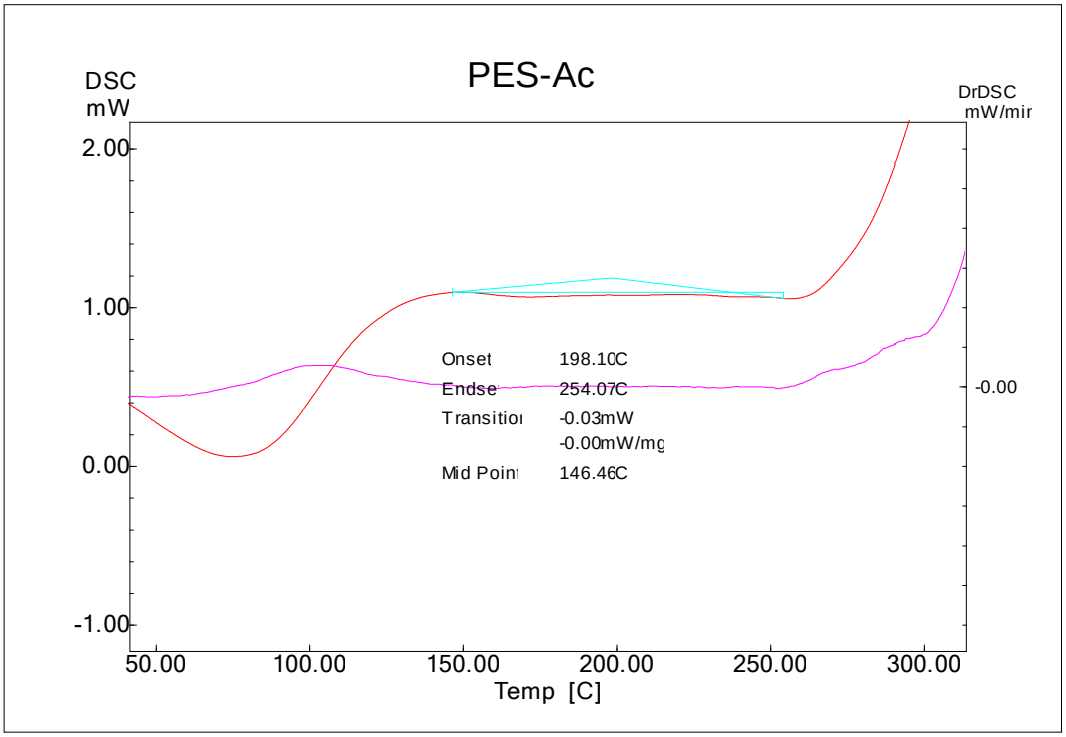

Figure 57. DSC graph of PES-NHAc.